

Characterization of *AtST10*, a sulfotransferase in *Arabidopsis thaliana*

Juan Francisco Leyva Illades

A thesis

In

The Department

Of Biology

Presented in Partial Fulfillment of the Requirements
for the Degree of Master of Science at Concordia University
Montréal, Québec, Canada

December, 2011

© Juan Francisco Leyva Illades

Concordia University
School of Graduate Studies

This is to certify that the thesis prepared

By: Juan Francisco Leyva Illades

Entitled: Characterization of *AtST10*, a sulfotransferase in *Arabidopsis thaliana*

and submitted in partial fulfillment of the requirements for the degree of

Master of Science (Biology)

complies with the regulations of the University and meets the accepted standards with respect to originality and quality

Signed by the final examining committee:

Dr. David Walsh

Chair

Dr. Reginald Storms

External Examiner

Dr. Patrick Gulick

Examiner

Dr. Paul Joyce

Examiner

Dr. Luc Varin

Thesis Supervisor

Approved by

Chair of Department or Graduate Program Director

_____ 2011

_____ Dean of faculty

Abstract

Characterization of *AtST10*, a sulfotransferase in *Arabidopsis thaliana*

Juan Francisco Leyva Illades

The relatively short life cycle and small size of *Arabidopsis thaliana* makes this plant a suitable model organism for biochemical and molecular biology studies. In our laboratory, we undertook the characterization of the 18 sulfotransferase-coding genes of this small flowering plant. This thesis describes the results of the biochemical and functional characterization of *AtST10*, one of these genes.

Probably the most interesting features of *AtST10* are its expression (restricted to the siliques, the plant's fruit) and the possibility of a miRNA regulating its expression in an indirect manner. We also demonstrate that the overexpression of *AtSt10* leads to a reduction in seed production to altered size compared with wild type plants suggesting that the *AtST10* substrate or product plays a role in seed development. Alternatively, *AtST10* might participate in the metabolism of another jasmonate, which is involved in seed development. Using a combination of different purification methods and mass spectrometry we identified the putative reaction product of the *AtST10*-catalyzed reaction. This molecule has a m/z of 307 Da in positive mode $[M+H]$ and generates fragments similar to the ones observed with 12-hydroxyjasmonate. Based on these results, we propose that the product of the reaction is the reduced form of 12-hydroxyjasmonate sulfate. This is the first report of the natural occurrence of this molecule in plants. Further experiments will be required to define the role of this metabolite or of its sulfonated product in seed development.

Acknowledgements

I would like to express my gratitude to my supervisor, Dr. Luc Varin, for allowing me to pursue my master's degree in his laboratory. I would also like to thank him for his guidance, patience and financial support, for it would have not been possible to achieve this without any of them. During my stay in his laboratory, I learnt more than just plant biology, and for that I am grateful as well. To my committee members, Dr. Patrick Gulick and Dr. Paul Joyce, I would also like to express my appreciation; their feedback during this process was most helpful.

I would also like to thank two other people external to Dr. Varin's laboratory: Alain Tessier and Dr. Detlef Weigel. Alain Tessier, from the Centre for Biological Applications of Mass Spectrometry (CBAMS), was of great help during the mass spectrometry experiments done in this study. Dr. Weigel, from the Max Planck Institute, made part of this work possible by providing the plasmid pRS300, which was used to construct an artificial micro RNA for the sake of this study.

I would also like to thank my friends for their support, encouragement, laughs, fun times and beers. This process would not have been the same without them; I owe them my sanity.

Lastly and most importantly, I would like to thank my family for their constant support and encouragement. Had I not had them, I would have not written these words.

A mi familia

Table of contents

List of figures	ix
List of tables	xi
List of abbreviations	xii
1. Literature Review	1
1.1 Introduction	1
1.2 Sulfotransferases	1
1.2.1 Introduction	1
1.2.2 Sulfotransferase nomenclature	3
1.2.3 Sulfotransferase structure	3
1.2.4 <i>Arabidopsis</i> sulfotranferases	5
1.2.5 <i>AtST10</i>	5
1.2.6 Micro RNA Regulation	6
2. Materials and Methods	8
2.1 Materials	8
2.2 Methods	8
2.2.1 Plant growth	8
2.2.2 Seed sterilization	8
2.2.3 RNA extraction methods	8
2.2.4 Regulation studies of <i>AtST10</i> expression	10

2.2.5 Molecular Cloning	12
2.2.6 Enzyme purification of recombinant AtST10	15
2.2.7 Enzymology	17
2.2.8 HPLC and mass spectrometry	18
2.2.9 Thin layer chromatography	19
2.2.10 Plant transformation	19
2.2.11 Expression study of transgenic plants.	20
2.2.12 Phenotype analyses	22
3. Results	23
3.1 Regulation of <i>AtST10</i> expression	23
3.2 Molecular cloning	25
3.2.1 <i>AtST10</i> overexpression	25
3.2.2 Expression of an artificial microRNA in transgenic <i>A. thaliana</i>	28
3.2.3 Cloning of <i>AtST10</i> in pQE30	32
3.3 Biochemical characterization of AtST10	32
3.3.1 Expression of recombinant AtST10 sulfotransferase	33
3.3.2 HPLC purification of AtST10 product and substrate	34
3.3.3 HPLC purification of AtST10 enzymatic reaction product	34
3.3.4 Thin layer chromatography of the AtST10 enzymatic product	35
3.3.5 Mass spectrometry	36
3.4 Morphometric analyses of the transgenic lines	44
4. Discussion	48

Future work

52

5. References

54

List of figures

Chapter 1

- Figure 1.1 General sulfonation reaction 2
- Figure 1.2 General miRNA pathway 6

Chapter 2

- Figure 2.1 Artificial miRNA cloning strategy 15

Chapter 3

- Figure 3.1 Expression level of *AtST10* at different stages of development 23
- Figure 3.2 RT-PCR of putative endogenous miRNA targeting the *AtST10* transcript 24
- Figure 3.3 Construct of transgenic *AtST10* overexpressor lines 25
- Figure 3.4 PCR amplification of *AtST10* overexpressing plants 26
- Figure 3.5 RT-PCR amplification of *AtST10* overexpressing plants 28
- Figure 3.6 Construct of *35S-35S::amiR-ST10* and hybridization region in *AtST10* transcript 29
- Figure 3.7 PCR amplification of artificial miRNA 30
- Figure 3.8 Artificial miRNA expression and function 31
- Figure 3.9 Construction of *AtST10* cDNA in pQE30 32
- Figure 3.10 Expression of recombinant protein in *E. coli* 33
- Figure 3.11 HPLC purification of radiolabeled enzymatic product 34
- Figure 3.12 TLC plate of recombinant *AtST10 in vitro* reaction products 35
- Figure 3.13 HPLC profiles of hydrolyzed TLC bands from 36

Arabidopsis siliques and *Brassica* seeds extracts

Figure 3.14 Mass spectra of silique extracts from wild type and transgenic *Arabidopsis* lines 38

Figure 3.15 Mass spectra of *Arabidopsis* and *Brassica* compounds purified from TLC plates 39

Figure 3.16 Activity of AtST10 using 12-hydroxyjasmonate as substrate 40

Figure 3.17 Mass spectra of compounds from various tissues purified from TLC plates 41

Figure 3.18 Neutral loss mass spectrometry of TLC-purified compounds from wild type and transgenic lines 43

Figure 3.19 Fragmentation pattern of the m/z 307 [M+H] molecular ion 44

Figure 3.20 Seed production of wildtype and *AtST10* transgenic lines 46

Figure 3.21 Seed volume of wildtype and *AtST10* transgenic lines 47

Chapter 4

Figure 4.1 Deduced chemical structures of 12-OHJA and its reduced form 51

List of tables

Table 1. Kanamycin resistance ratios of <i>AtST10</i> overexpressing lines	26
Table 2. Relative abundance of the m/z305 [M+1] and m/z 307 [M+1] molecular ions among different <i>Arabidopsis</i> transgenic lines	42

List of abbreviations

ABH1	ABA HYPERSENSITIVE 1
AGO	ARGONAUTE
AMV	Alfalfa Mosaic Virus
<i>AtST10</i>	<i>Arabidopsis thaliana</i> sulfotransferase 10
bp	Base pair
Col-0	Columbia 0
CPM	Counts per minute
DCL1	<i>DICER-LIKE 1</i>
DEPC	Diethylpyrocarbonate
dsRNA	Double stranded RNA
EDTA	Ethylenediaminetetraacetic acid
HEN1	HUA ENHANCER
HPLC	High performance liquid chromatography
HYL1	HYPONASTIC LEAVES 1
JA	Jasmonic acid
12-OHJA	12 hydroxyjasmonic acid
kb	Kilobase pair
kDa	Kilodalton
LC	Liquid chromatography
miRNA	Micro RNA
MS	Mass spectrometry
MS/MS	Tandem mass spectrometry

PCR	Polymerase chain reaction
RT	Reverse transcriptase
SE	SERRATE
SULT	Sulfotransferase
TBS	Tris-buffered saline
TLC	Thin layer chromatography
TTBS	Tween Tris-buffered saline

1. Literature Review

1.1 Introduction

In this first chapter I review the main topics related to the characterization of the *AtST10* sulfotransferase gene and protein from *Arabidopsis thaliana*. A brief presentation of sulfotransferases (SULTs) comes first, reviewing their nomenclature, structure and function, with emphasis on plant cytosolic SULTs. Also, I am introducing miRNA regulation, a form of posttranscriptional gene regulation, which might have a role in the expression of the *AtST10* gene of *A. thaliana*.

1.2 Sulfotransferases

1.2.1 Introduction

SULTs are enzymes present in animals as well as in plants that play important roles in the detoxification of xenobiotics and in the control of hormone activity (Weinshilboum and Otterness, 1994; Yasuda *et al.*, 2005). In *Arabidopsis thaliana* there are 18 SULT-coding genes, eight of which have been characterized. The gene products are divided into different subfamilies according to amino acid sequence comparison. SULTs are enzymes that catalyze the transfer of a sulfonate group to an acceptor molecule. The sulfonate group is provided by the ubiquitous donor 3'-phosphoadenosine 5'-phosphosulfate (PAPS) and transferred to the appropriate hydroxyl group of a variety of molecules; the products of the reaction are adenosine 3',5'-diphosphate and a sulfuric acid ester (Nimmagada, *et al.*, 2006) (Figure 1.1). This biochemical process is known as sulfonation and it takes place in the cytosol or membranes of the Golgi apparatus. There are two classes of SULTs: cytosolic SULTs, which carry out the sulfonation of small endogenous and exogenous compounds, such as hormones

and xenobiotics; and membrane associated SULTs, which sulfonate larger biomolecules, such as complex carbohydrates and proteins. The cytosolic enzymes have highly conserved domains and are found in animals, plants and bacteria (Hernández-Sebastiá, *et al.*, 2008).

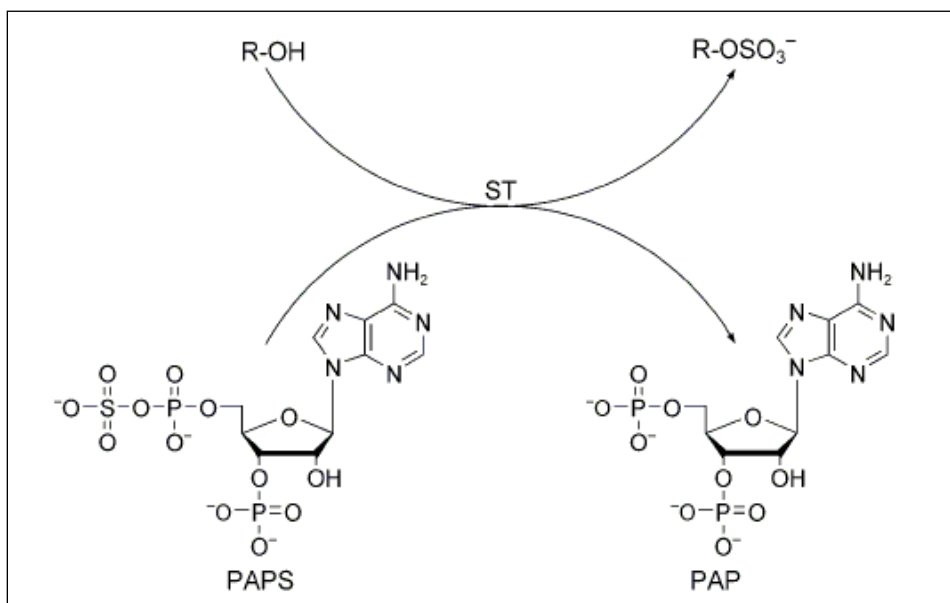


Figure 1.1. General sulfonation reaction catalyzed by SULTs, where PAPS donates an SO₃ group to an acceptor molecule (Chapman *et al.*, 2004).

The sulfonation reaction seems to be of great importance in life, as it can be found in several biological processes where the effects of the reaction have several outcomes. The addition of a sulfonate group to a molecule makes it more polar and water soluble, thus resulting in enhanced excretion. For example, mammalian SULTs have a fundamental role in phase II of biotransformation and excretion of xenobiotics from the liver (Weinshilboum and Otterness, 1994; Yasuda *et al.*, 2005). The sulfonation reaction also regulates the biological activity of some metabolites such as steroids. For example, the sulfonation and desulfonation reactions control the level of active estrogen in the blood of mammals. Sulfated estrogen acts as an

estrogen storage pool and eventually is converted to the active hormone after removal of the functional group by sulfatases (Strott, 1996). Also, the sulfonation reaction can increase the biological activity of some metabolites. For example, the sulfonation of tyrosine residues on the chemokine receptor CCR5 (a principal HIV-1 co-receptor) is a modification that is required for its biological activity and indirectly facilitates entry of HIV-1 (Farzan *et al.*, 1999).

In plants, SULTs play roles in the regulation of plant growth, defense and stress responses. For example, it has been shown that the sulfonation of desulfoglucosinolate is required for the activation of the antimicrobial properties of glucosinolates (Piotrowski *et al.*, 2004; Klein *et al.*, 2006). Moreover, the choline sulfate that accumulates under saline conditions is involved in salt or drought stress-tolerance in *Limonium* species and other plants of the Plumbaginaceae family (Rivoal and Hanson, 1994)

1.2.2 Sulfotransferase nomenclature

An effort by Blanchard *et al.* (2004) to classify SULTs defines members within a family share more than 45% amino acid sequence identity, whereas members of the same subfamily share more than 60% amino acid sequence identity. In *Arabidopsis*, sulfotransferases have been classified into four families: SULT201, SULT202, SULT203 and SULT204.

1.2.3 Sulfotransferase structure

The solved X-ray crystal structures of six cytosolic SULTs from humans and mice revealed that they are globular proteins with an α/β fold and 4-5 parallel β -sheets surrounded by α -helices. The β -sheet constitutes the PAPS-binding site and the core of the catalytic site, both of which are conserved in cytosolic as well as membrane-bound SULTs. The largest variation

among these enzymes is found in the substrate-binding region (Nimmagadda *et al.*, 2006; Negishi *et al.*, 2001). The amino acid sequence comparison of SULTs of plant and animal origin has suggests a high level of homology, which led to the identification of four well conserved regions named I, II, III and IV (Weinshilboum *et al.*, 1997; Klein and Papenbrock, 2004; Hernández-Sebastiá *et al.*, 2008).

Experimental evidence suggests that regions I and IV are involved in PAPS binding (Weinshilboum *et al.*, 1997; Klein and Papenbrock, 2004; Hernández-Sebastiá *et al.*, 2008). There are two structural motifs involved in this process: the 5'-phosphosulfate-binding motif (PSB-loop) near the N-terminus of region I; and the 3'-phosphate binding sequence (PB-loop), located in region IV (amino acids RKG). Sequence comparisons have shown that the consensus sequence in the PAPS-binding regions of SULTs from *Arabidopsis thaliana* are PKxGTTWLKALTFA and FRKGxVGDWxxxLT for region I and IV, respectively (Hernández-Sebastiá *et al.*, 2008; Klein and Papenbrock, 2004).

In contrast to the highly conserved PAPS-binding site, the substrate binding site of each of these enzymes has certain differences that define their substrate specificity. Analysis of substrate preference in flavonol sulfotransferases showed that region II contains the amino acids for substrate recognition, which flank a highly conserved region (Varin *et al.*, 1995).

Apart from the PAPS-binding regions and the substrate-binding site, there is a third domain; the catalytic site, responsible for the transfer of the sulfonate to the substrate. Site-directed mutagenesis studies demonstrated the critical role of the Lys⁵⁹ residue in region I of the a flavonol 3 sulfotransferase in *Flaveria chloraefolia* for catalysis and of a strictly conserved histidine residue located in at the interface between region II and III. Substitution of Lys⁵⁹ with

the amino acids Arg and Ala resulted in a decreased specific activity (15-fold and 300-fold, respectively) without affecting PAPS-binding (Marsolais and Varin, 1995, 1998).

1.2.4 *Arabidopsis* sulfotranferases

A. thaliana, whose genome was completely sequenced in 2001, is a small flowering plant with a relatively short life cycle; characteristics which make it a suitable model organism in plant molecular biology.

The fully sequenced genome of *A. thaliana* contains 18 SULT-coding genes including one pseudogene (Hernández-Sebastià *et al.*, 2008). Eight of these genes have been characterized: Flavonoid SULT *At3g45070* (Gidda and Varin, 2006); desulfoglucosinolate SULTs *At1g74100*, *At1g74090*, *At1g18590* (Piotrowski *et al.*, 2004); hydroxyjasmonate SULTs *At5g07010* (Gidda *et al.*, 2003); brassinosteroid SULTs *At2g03760* and *At2g14920* (Marsolais *et al.*, 2004); and cadabicine SULT *At1g13420* (Khodashenas, 2010).

1.2.5 *AtST10*

Based on the proposed guidelines of Blanchard *et al.* (2004), *AtST10* is part of the SULT204 subfamily. Interestingly, *AtST10* (*At1g28170*) is the only *A. thaliana* member of this subfamily. The locus is located on chromosome 1 of the *Arabidopsis* genome.

Microarray data has shown that *AtST10* expression is induced following the exogenous application of gibberellic acid. The expression is also increased in a *serrate* mutant, a gene involved in the maturation of micro RNA (Genevestigator).

1.2.6 Micro RNA Regulation

Small non protein-coding RNAs play diverse roles in cell biology. Reverse transcription, developmental regulation, epigenetic modifications, RNA splicing, tumorigenesis, stress response, protein synthesis, chromatin modification and gene silencing are well known examples (Mallory *et al*, 2008).

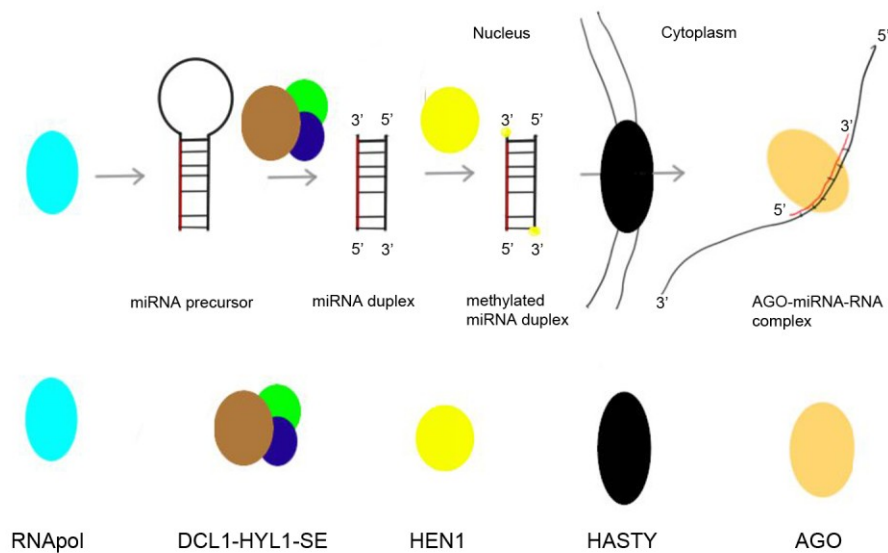


Figure 1.2. General miRNA pathway. The miRNA sequence is represented in red.

Micro RNAs (miRNA) are short, non-coding single stranded RNA molecules which down regulate gene expression by hybridizing to other coding mRNA molecules. This process, which is mediated by a series of proteins, causes degradation of the target mRNA (Figure 1.2). This type of nucleic acid starts as a partially double stranded hairpin fold that is typical of all known miRNAs (Bartel, 2004). In *Arabidopsis*, miRNA transcripts are processed by the ribonuclease III enzyme DCL1 assisted by the double stranded RNA (dsRNA) binding protein

HYPONASTIC LEAVES1 (*HYL1*) and the zinc finger containing SERRATE protein (*SE*). Together, these two enzymes liberate a single 21 base pair miRNA duplex (Ramachandran and Chen, 2008). It has been demonstrated that plants expressing *se-1*, a seven base pair deletion mutant of *SE*, have a decreased accumulation of several known mature miRNAs such as *MIR156*, *MIR159*, *MIR163*, *MIR164*, *MIR165*, *MIR167*, *MIR168*, *MIR171* (Lobbes *et al*, 2006). Moreover, it has been shown that ABA HYPERSENSITIVE1 (*ABH1*) is required for proper miRNA precursor processing. (Yang *et al*, 2006; Laubinger *et al*, 2008; Gregory *et al*, 2008). After the excision mediated by the DCL1-HYL1-SE complex, the small RNA is methylated at its 3' end. HUA ENHANCER (*HEN1*) possibly does this methylation, but it is unclear (Ramachandran and Chen, 2008). HASTY exports the RNA either as a single or duplex strand to the cytoplasm where one strand of the miRNA duplex associates with one of the ten *Arabidopsis* ARGONAUTE (*AGO*) proteins which subsequently carries on with the cleavage and transcriptional repression of partially complementary mRNAs (Chapman and Carrington, 2007; Vaucheret, 2006; Mallory and Bouché, 2008). Microarray data have shown that *se-1* causes *AtST10* to be overexpressed in *Arabidopsis*, suggesting a role of this type of nucleic acid in the regulation of the mentioned sulfotransferase.

The specificity in time and space of the expression of *AtST10* makes it an interesting gene for study. The aim of this study was to characterize the biological and biochemical roles of this sulfotransferase. Gene expression measurements, phenotype analyses of transgenic plants affected in *AtST10* expression and mass spectrometry were the tools used for this purpose.

2. Materials and Methods

2.1 Materials

Wild type seeds of *A. thaliana* were obtained from Lehle seeds (USA). All experiments with wild type and transgenic plants were performed in a Col-0 background. *Agrobacterium tumefaciens* strain GV3101 was used to transform wildtype *Arabidopsis* plants. XL1-blue, a strain of *Escherichia coli*, was used to harbour the *AtST10* recombinant coding sequence.

2.2 Methods

2.2.1 Plant growth

The plants were grown either in soil or on Petri dishes containing Murashige and Skoog (MS) medium with 1% sucrose, 0.4% Gelrite, 0.05% MES, pH 5.7, under long day conditions (16 h of light and 8 h of dark). Temperature was kept at 22°C for the duration of the light and dark periods. Seeds to be sown in soil were left at 4°C for 2 to 4 days to improve germination.

2.2.2 Seed sterilization

Arabidopsis seeds that needed to be grown in MS medium were surface sterilized by immersion in 70% ethanol for 30 seconds, followed by 5 minutes of vigorous shaking in a sterilizing mix (10% bleach and 0.02% SDS) and rinsing 4 times in sterile distilled water sterilized prior to sowing. The seeds were then kept 2 to 4 days at 4°C.

2.2.3 RNA extraction methods

Three methods for RNA extraction were used. One was meant for expression studies of

AtST10 in wild type and overexpressing lines; the second also was used for expression analyses of *AtST10*, but in siliques; while the third was done for detection of micro RNAs. The first was carried out using the plant RNA easy kit (Qiagen, U.S.A.) following the manufacturer's instructions and treating with DnaseI as described in the protocol. RNA from siliques and seeds was extracted as described by (Oñate-Sánchez and Vicente-Carbajosa, 2008).

Seeds and silique tissues have a high content of polysaccharides, which contaminate the RNA samples, justifying the choice of a different method for extracting RNA. The tissue was first ground to a fine powder in liquid nitrogen and transferred to a microfuge tube, where it was mixed with 550 µl of extraction buffer (0.4 M LiCl, 0.2 M Tris pH 8, 25 mM EDTA, 1% SDS) and 550 µl chloroform, and then centrifuged for 3 minutes. The resulting supernatant was transferred to a new tube, 500 µl of water saturated acidic phenol was added, vortexed and an additional 200 µl of chloroform were added. After 3 minutes of centrifugation at 12,000Xg, the supernatant was transferred again to a new tube; the volume was increased with 1/3 of volume of 8 M LiCl and mixed. The mixture was left to precipitate for 1 h at -20°C, followed by 30 minutes of centrifugation at 4°C. The samples were treated with DNase I (Roche, Germany) for 30 minutes at 37°C by dissolving the pellet in 26 µl of DEPC-water, 3 µl of 10X DNase I buffer and 1 µl of the enzyme. The volume was brought to 500 µl with DEPC-water, 7 µl of 3 M sodium acetate (pH 5.2) and 250 µl of ethanol were added with thorough mixing and centrifugation for 10 minutes at 4°C to precipitate the carbohydrates. The supernatant was transferred to a new tube, where 43 µl of sodium acetate (pH 5.2) and 750 µl of ethanol were added and then left 1 h at -20°C. The tubes were centrifuged again for 20 minutes at 4°C, the pellet washed with 70% ethanol and the air-dried RNA was resuspended in 20 µl of DEPC-water.

Since the mini columns are not suitable for the extraction of miRNAs, the isolation of these RNAs was carried out using the TRI reagent (Sigma, U.S.A.). The plant tissue was ground in liquid nitrogen and resuspended in 1 ml of TRI reagent per 100 mg of tissue. After five minutes at room temperature, 200 µl of chloroform was added per 1 ml of TRI reagent and vortexed vigorously. A subsequent 3 minute incubation was carried out at room temperature, followed by 15 minutes of centrifugation at 12,000Xg at 4°C. The top phase was transferred to a new tube and precipitated with 500 µl of isopropanol per 1 ml of TRI reagent, incubating at room temperature for 10 minutes followed by 10 minutes of centrifugation at 4°C at 12,000Xg. The supernatant was removed and the pellet washed twice with 1 ml of 75% ethanol per 1 ml of TRI reagent and centrifuged at 4°C at 7,500Xg. The resulting pellet was left to air-dry and resuspended in DEPC-treated water.

2.2.4 Regulation studies of *AtST10* expression

- *AtST10* expression at different stages of development

For reverse transcription polymerase chain reaction (RT-PCR) experiments, 2 µg of total RNA was used. A PCR master mix containing (per reaction) 2 µl of 10x Thermopol buffer (NEB, U.S.A.), 1.7 µl of 2.5 mM dNTP mix (NEB, U.S.A.), 2 µl of 4 µM of each forward and reverse primers, 0.3 µl of Taq DNA polymerase 5,000 U/µl (NEB, U.S.A.) and 10 µl of water was made for both *AtST10* and Actin, which was used as a positive and internal control. The primers used for the *AtST10* reactions had the sequences 5'-ATG GAT GAG ACC AAG ATC CCA-3' and 5'-TCA GAA TTT CAA ATC CGA ACC TTC AAA-3'. The thermocycling program was set for 30 cycles (45 s at 94 °C, 45 s at 60 °C, 1 minute at 72°C) with an initial denaturation of 5 minutes at 94°C and a final extension of 7 minutes at 72°C. For Actin amplification, the same

program was used, but with only 25 cycles. A PCR reaction with genomic DNA was used as a control to monitor DNA contamination of the RNA samples. The Actin primers were designed to span an intron generating products of different sizes using DNA or cDNA samples. The PCR program was used first with the Actin primers for cDNA calibration. The volumes of cDNA were adjusted after calibration based on the intensity levels of the Actin PCR products.

- Endogenous miRNA detection

An attempt to detect hypothetical, naturally occurring micro RNA was carried out by RT-PCR as described by Varkonyi-Gasic, *et al* (2007). Total RNA was extracted from 4, 8, 12, 16, 20, and 24 day old whole plants, dissected flowers, siliques or seeds. A 'no RT primer' master mix was prepared by mixing 0.5 µl of 10 mM dNTP, 11.15 µl of nuclease-free water and 1 µl of RNA. The mixture was heated at 65 °C for 5 minutes and incubated on ice for 2 minutes. After a brief centrifugation, 4 µl of 5x first-strand buffer was added (Invitrogen, U.S.A.), along with 2 µl of 0.1 M DTT, 0.1 µl of RnaseOUT (Invitrogen, U.S.A.) and 0.25 µl of Superscript III RT (Invitrogen, U.S.A.). To assemble the RT reaction, 19 µl of the RT master mix were transferred to a new tube, 1 µl of sample RNA was added (20 ng), as well as the appropriate RT primer (10 µM). Following the assembly, a pulsed RT was performed. For this purpose, the samples were incubated in a thermocycler at 16°C for a period of 30 minutes, followed by 60 cycles of 30°C for 30 seconds, 42°C for 30 seconds and 50°C for 1 s. Finally, the samples were incubated at 85°C for 5 minutes to inactivate the reverse transcriptase. The subsequent PCR reaction was carried out for each sample, by adding 15.4 µl of nuclease-free water, 2 µl of 10x PCR buffer, 0.4 µl of 10 mM dNTP mix, 0.4 µl of forward primer (10 µM), 0.4 µl of reverse primer (10 µM) and 0.4 µl of Platinum Taq HI-FI (Invitrogen, U.S.A.). An aliquot of 19 µl PCR mix was added to 1 µl of RT product and the thermocycler was set at 94 °C for 2 minutes,

followed by 40 cycles of 94°C for 15 seconds and 60°C for 1 minute. The final PCR products were analysed in a 7% polyacrylamide gel. The oligonucleotides used for this experiment are listed below. miR159 was used as a positive control.

Endogenous miRNA RT primer

5'- GTCGTATCCAGTGCAGGGTCCGAGGTATTTCGCACTGGATACGACGCTCTC -3'

miR159 RT primer

5'- GTCGTATCCAGTGCAGGGTCCGAGGTATTTCGCACTGGATACGACTAGAGC-3'

Endogenous miRNA forward primer

5'- GCGGCGGTTGGATCAGTTGAG -3'

miR159 forward primer

5'- CGGCGGTTTGGATTGAAGGGA -3'

miRNA reverse primer

5'- GTGCAGGGTCCGAGGT -3'

2.2.5 Molecular Cloning

- Cloning of the AtST10 coding sequence

For the biochemical characterization of *AtST10* and its overexpression in plants, its coding sequence was cloned into the bacterial expression vector pQE30 (Qiagen, U.S.A) and the plant transformation vector pRD525, respectively. The primers used to generate fragments for

cloning in the plasmids are listed below. *AtST10* was amplified using the primers 1 and 2 for directional cloning into the *BamHI* and *SphI* sites of pQE30, whereas primers 3 and 4 were used to clone into the *XbaI* and *BamHI* sites of pRD525. Since it lacks introns, the gene was amplified from genomic DNA in both cases. The amplification was done using Pfu DNA polymerase 2.5 U/μl (Stratagene, U.S.A). All PCR products were first cloned in pJet using the CloneJet kit (Fermentas, Lithuania) following the manufacturer's instructions.

Primers

- 1- *AtST10* FWD pQE30: 5'- GGGGATCCATGGATGAGACCAAGATCCCA -3'
- 2- *AtST10* REV pQE30: 5'- GGGCATGCTCAGAATTTCAAATCCGAACCTTCAAAA -3'
- 3- *AtST10* FWD pRD525: 5'- GGTCTAGAATGGATGAGACCAAGATCCCA -3'
- 4- *AtST10* REV pRD525: 5'- GGGGATCCTCAGAATTTCAAATCCGAACCTTCAAAA -3'

- Cloning of artificial miRNA

Due to the absence of a T-DNA knockout line of *AtST10*, an artificial micro RNA (amiR) targeting specifically *AtST10* was cloned into the *BglII* and *XbaI* sites of pRD525 and named 35S-35S::amiR-*ST10*. The design of the amiR was done using the guidelines provided by Weigel *et al* (<http://wmd3.weigelworld.org>). The designer gave an output of 36 sequences and the sequence 5'-TAA AAC GAC ACC AGT ACG CCT-3' was selected. The six oligo sequences for cloning the amiR, which are listed below, were obtained by using the oligo designer in the available webpage. However, the sequence of oligo A was changed in order to introduce a *BglII* site. Figure 2.1 shows a diagram of the artificial miRNA cloning strategy, with the location (in the plasmid) of the complementary sequences of the oligos used. The overlapping PCR amplification was carried out in two steps. First, three separate reactions

were done using pRS300 as template and labelled as a, b and c. Plasmid pRS300 is a plasmid provided by Dr. Detlef Weigel which contains the backbone sequence of MIR139a (Max Planck Institute for Developmental Biology, Tübingen, Germany). All three reactions contained 5 µl of 10xPCR buffer, 5 µl of 2 mM dNTP, 2 µl of template, 0.5 µl of Pfu 2.5 U/µl (Stratagene, U.S.A), 33.5 µl of water and 2 µl of each oligo (2.5 mM). The oligos varied in the three reactions: a used oligos A and IV; b used oligos III and II; and c used oligos I and B. The thermocycler was set for 30 cycles comprising 30 s at 95°C, 30 s at 55°C, 40 s at 72°C, an initial denaturation of two minutes at 95 °C and a final extension of seven minutes at 72°C. The bands were separated by electrophoresis and extracted from the gel using the QIAquick Gel Extraction Kit (Qiagen, U.S.A). A second step (reaction d) was done using the PCR products of reactions a, b and c. The mix contained 5 µl of 10X PCR buffer, 5 µl of 2 mM dNTP, 0.5 µl of each previous product, 0.5 µl of Pfu 2.5 U/µl (Stratagene, U.S.A), 2 µl of oligo A, 2 µl of oligo B and 34.5 µl of water. In this case the thermocycler was set also for 30 cycles, but 30 s at 95°C, 30 s at 55 °C, 1.5 minutes at 72°C, an initial denaturation of two minutes at 95 °C and a final extension of seven minutes at 72°C. The resulting product was cloned into pJet (Fermentas, Lithuania) and sequenced. Due to the existence of two *BglII* sites in pRD525, the product was cloned first into the *BglII* and *XbaI* sites of pBI525 and then the cassette containing the promoter, amiR backbone and terminator sequence was cloned into the *HindIII* and *EcoRI* sites of pRD400.

Oligos:

I. 5'-GAT AAA ACG ACA CCA GTA CGC CTT CTC TCT TTT GTA TTC C-3'

II. 5'-GAA GGC GTA CTG GTG TCG TTT TAT CAA AGA GAA TCA ATG A-3'

III. 5'-GAA GAC GTA CTG GTG ACG TTT TTT CAC AGG TCG TGA TAT G-3'

IV. 5'-GAA AAA ACG TCA CCA GTA CGT CTT CTA CAT ATA TAT TCC T-3'

A. 5'-GAA **GAT CTC** TGC AGC CCC AAA CAC ACG-3'

B. 5'-GCG GAT AAC AAT TTC ACA CAG GAA ACA G-3'

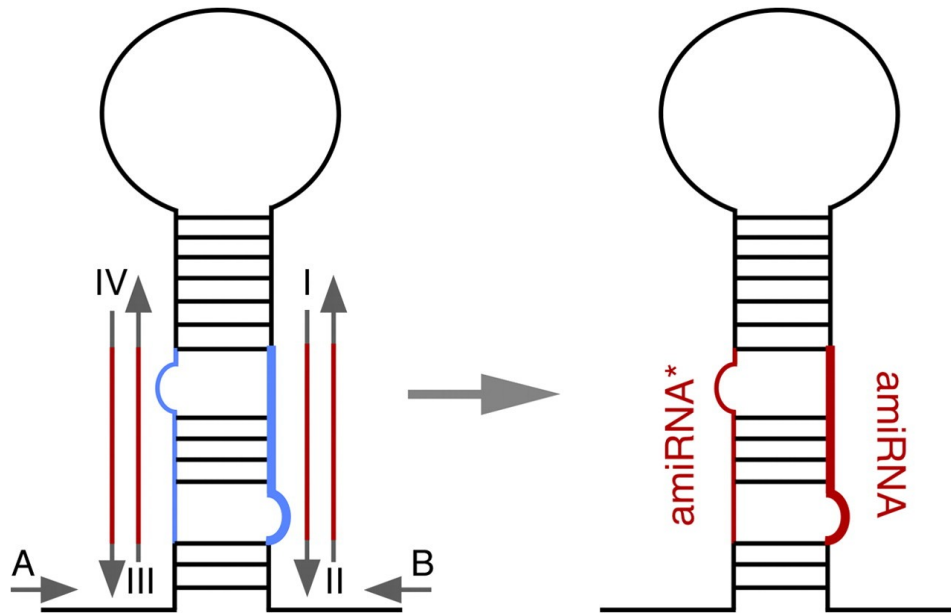


Figure 2.1. Artificial miRNA cloning strategy. Image on the left shows the sites where all six oligo sequences align (gray sections of the arrows), as well as the overlapping regions among them (shown in red), resulting in a region in the plasmid pRS300 as the one shown on the right.

Source: Scwabb, *et. al.* 2006

2.2.6 Enzyme purification of recombinant AtST10

In order to check that the enzyme was being produced in *E. coli*, it was purified using a Ni-NTA agarose affinity column (Qiagen, U.S.A.). First, 3 ml of LB medium supplemented with ampicillin (50 µg/ml) was inoculated with a single *E. coli* colony harbouring the *AtST10* construct and left to grow overnight at 37°C. On the second day, 100 ml of LB medium supplemented with ampicillin (50 µg/ml) was inoculated with 100 µl of the subculture, induced with 1 mM IPTG and left to grow overnight at 20°C. On the third day, the culture was centrifuged at 8,000 revolutions per minute (rpm) for 20 minutes at room temperature,

resuspended in 7 ml of lysis solution (50 mM NaH₂PO₄, 30 mM NaCl, 10 mM Imidazole) and sonicated on ice (10 s with 15 s intervals for total of 5 minutes) to break down the cells. The lysate was centrifuged again at 10,000 rpm for 20 minutes at 4°C and the supernatant was transferred to a 15 ml conical tube containing the Ni-NTA agarose matrix (previously equilibrated in lysis buffer) and left to bind for 1h with gentle shaking at 4°C. The tube was centrifuged at 7,000 rpm to collect the matrix and the supernatant discarded, then two washes with 7 ml of wash buffer (50 mM NaH₂PO₄, 30 mM NaCl, 20 mM Imidazole) were carried out, followed by three elutions with 300 µl of elution buffer (50 mM NaH₂PO₄, 30 mM NaCl, 250 mM Imidazole). The proteins were then separated on a polyacrylamide gel. First, a Bradford assay –using BSA as a reference- was carried out to quantify the proteins. A total of 25 µg for total crude protein was aliquoted and 5 µg of purified protein. The samples were boiled for 5 minutes at 95°C in sample buffer (50 mM Tris-HCl pH 6.8, 2% SDS, 10% glycerol 1% β-mercaptoethanol, 12.5 mM EDTA, 0.02% bromophenol blue) and later loaded in a polyacrylamide gel (12% resolving, 4% stacking at 150 V) followed by staining with Coomassie blue for 30 min.

A Western blot was also carried out. A second polyacrylamide gel was run under the same conditions and then transferred to a nitrocellulose membrane using the wet transfer method: the gel was stripped from the plate and placed in direct contact with a nitrocellulose membrane, in between blotting paper. The resulting left to transfer in transfer buffer (25 mM Tris, 192 mM glycine, 10% methanol) for 1 h at 100 V. The membrane was later stripped and blocked for 1 h at room temperature with 10 ml of blocking solution (1x TBS, 5% powdered milk, 0.1% Tween-20) with gentle shaking. The primary antibody, a polyclonal antibody against AtST2a previously generated in rabbits, was added at a concentration of 1:1000 and left to bind for 1h at room temperature. The membrane was then washed three times with

TTBS (0.1% Tween-20, TBS) for ten minutes each time. The membrane was covered with 10 ml of a solution containing 1:3000 goat anti-rabbit secondary antibody (Bio-Rad, U.S.A.), and left to bind for 1 h at room temperature. The membrane was washed two times with TTBS, one time with TBS and then developed with the AP conjugate developing kit from Bio-Rad (U.S.A.) following the manufacturer's instructions.

2.2.7 Enzymology

- Metabolite extraction

Siliques from *Arabidopsis thaliana* were collected, weighed, frozen in liquid nitrogen and ground to a fine powder. A mix of 50:50 water:methanol was added at 3 ml per gram of tissue, and mixed thoroughly at room temperature. After one hour of mixing (with a magnetic mixer), the mixture was centrifuged for 15 minutes at 10,000 rpm at 4°C. The supernatant was collected and transferred to a round bottom flask, which was connected to a Rotovapor R114 (Büchi, Germany) and the volume reduced until it reached 50% of the original volume of the water:methanol mix. The extract was transferred to Corex tubes and an equal volume of butanol was added and subsequently mixed and centrifuged. The upper layer, containing the sulphated compounds in butanol, was divided into several 2 ml microfuge tubes, depending on the volume, where each 1.5 ml of butanol represented one gram of tissue. The samples were later lyophilised in a speed vacuum at room temperature overnight.

- Enzymatic assays

For the purpose of enzymatic assays, the recombinant AtST10 was extracted from *E. coli* cells harbouring the plasmid. The steps for extraction were basically the same as the first section of purification prior to binding to the column, but the first buffer was changed to 50 mM

Tris-HCl (pH 7.5) with 1:1000 β -mercaptoethanol. After sonication and centrifugation, the supernatant was collected and kept on ice to be used directly for enzyme assays. Radiolabeled PAPS was used to perform the enzyme assays. First it was diluted by mixing 10 μ l of the PAPS stock in 500 μ l of 50 mM Tris-HCl (pH 7.5). Each assay was done in a total volume of 40 μ l by mixing 5 μ l of the diluted radiolabeled PAPS, 5 μ l of the plant metabolite extract (lyophilized extract previously dissolved in 100 μ l of 50% MeOH) and 40 μ l of the total enzyme extract in a 1.5 ml microfuge tube. After 10 minutes at room temperature, the reaction was stopped by the addition of 10 μ l of 2.5% acetic acid, and then the radiolabeled product was extracted with 200 μ l of ice-cold water saturated butanol. After mixing and centrifugation, 100 μ l of the top layer was transferred to a scintillation vial with 2 ml of scintillation fluid for radioactivity measurements.

In some cases the assays were done with crude metabolite extracts, while in others they were carried out using individual fractions after reverse phase HPLC purification.

2.2.8 HPLC and mass spectrometry

The extracted metabolites were purified using an Agilent 1200 series HPLC (Agilent Technologies, U.S.A) and a Spursil 3 μ m 150 x 1.2 mm C18 column (Dikma Technologies, U.S.A.; catalogue no: 82013; serial no: 2201977). The mobile phase consisted of solvents A (H₂O, 5 mM ammonium acetate, 0.05% acetic acid) and B (100% methanol, 5 mM ammonium acetate, 0.05% acetic acid), and the elution was done at a flow rate of 200 μ l/min with the following method: 5 minutes in 100% of A; 50 minutes from 100% A and 0% B to 0% A and 100% B; and finally 5 minutes in 100% B, for a total of a 60 minute run. Fractions corresponding to one minute elution were collected. For mass spectrometry experiments, the

HPLC was connected to a Quattro-LC (Waters, U.S.A.) for LC-MS, LC-MS; the scans were done from 200 to 800 Da.

2.2.9 Thin layer chromatography

Approximately 10,000 CPM of radioactive product from the reaction of AtST10 and extracts from wild-type *A. thaliana* siliques and *Brassica napus* seeds were spotted on a cellulose plate and left to separate for three hours in a TLC chamber containing 200 ml of mobile phase which contained butanol, acetic acid and water (6:2:2). The plate was left to dry and exposed to a phosphor screen.

Non-hydrolysed extracts from wild-type *Arabidopsis thaliana* siliques and *Brassica napus* seeds were spotted on a cellulose TLC plate with 10,000 CPM from the reaction product of AtST10 and a silique extract. The samples were left to separate in a TLC chamber as described above. After three hours the plate was air dried, exposed to a phosphor screen and developed on a Typhoon Trio (General Electric Healthcare, U.S.A). The distance travelled by the analyte was measured and the band corresponding to the non-hydrolysed spot was excised and extracted with 50% methanol. The extract was lyophilized and resuspended in 50% methanol with 5 mM ammonium acetate and scanned for a neutral loss of 80 on the Quatro mass spectrometer. The same procedure was carried out for extracts of *AtST10* overexpressor line, *35S-35S::amiR-ST10* and *B. napus* extracts.

2.2.10 Plant transformation

Agrobacterium tumefaciens was transformed by electroporation with pRD525 harbouring *AtST10* or *35S-35S::amiR-ST10* and plated on LB agar supplemented with 50 µg/ml of

Gentamycin and Kanamycin. A colony of each transformation was selected and grown in LB medium with the mentioned antibiotics for ~16 h and on the next day one litre of medium was inoculated with 1 ml of the pre-culture. The cultures were centrifuged and then diluted to an OD₆₀₀ of 0.8 in fresh 5% sucrose solution with 0.002% Silwet-77. The plants, clipped 2 days before transformation, were dipped and shaken gently in the solution for two to three seconds, making sure that the axillary buds were fully immersed. The plants were covered to maintain humidity for a few days and left to grow until seed collection. All seeds (T₀ seeds) of each plant were pooled, surface sterilized and spread on MS medium supplemented with 100 µg/ml of kanamycin, given that pRD525 confers resistance to this drug. Resistant T₁ plants were transferred to soil and seeds (T₂ seeds) were collected afterwards. T₁ seeds, 50 of each transformed plant, were grown in MS medium with kanamycin to search for single insertion mutants by assessing kanamycin resistance ratios. Resistance to the drug was determined by growth and colouration of the plants; those green and with long roots were considered to be resistant, whereas those white and/or with a poorly developed root were considered to be sensitive. T₂ seeds of these plants were also grown on MS medium with kanamycin to search for homozygous plants.

2.2.11 Expression study of transgenic plants.

- Expression study of *AtST10* in overexpressor and *35S-35S::amiR-ST10* lines

Total RNA was extracted from root and leaf tissue of *AtST10* overexpressor lines using the Plant RNA mini kit (Qiagen, U.S.A.). RNA from siliques was extracted for the study of *AtST10* expression in the *35S-35S::amiR-ST10* line. Total RNA (2 µg) was used for RT-PCR, using Actin primers as internal control. The PCR conditions were the same as those described in section 2.2.4.

- Expression study of 35S-35S::amiR-ST10

Total RNA was extracted from plant tissue as explained in the RNA extraction section. RT-PCR experiments were carried out as described in the Endogenous miRNA detection section. In this case, since the expression of the artificial micro RNA was constitutive, leaf tissue was used. Also, miR159 was used as a positive control. The primer sequences used were the following:

miR159 RT primer

5'- GTCGTATCCAGTGCAGGGTCCGAGGTATTCGCACTGGATACGACGTGCTC -3'

amiR-ST10 RT primer

5'- GTCGTATCCAGTGCAGGGTCCGAGGTATTCGCACTGGATACGACAGGCGT -3'

miR159 forward primer

5'- CGGCGGTTTGGATTGAAGGGA -3'

amiR-ST10 forward primer

5'- CGGCGGTAAAACGACACCAGT -3'

miRNA reverse primer

5'- GTGCAGGGTCCGAGGT -3'

2.2.12 Phenotype analyses

Given that the expression of *AtST10* is at its highest in siliques, phenotypic analyses were focused on this tissue. Seeds and siliques from wild type, artificial miRNA and overexpression lines were analysed using a Nikon microscope coupled to a Leica digital camera. Measurements of seed length and width were done using the Leica Suite 3.0 software. Statistical analyses (Tukey's HSD test) were done on seed sizes and the number of seeds per silique in all genotypes.

3. Results

3.1 Regulation of *AtST10* expression

In order to study the regulation of *AtST10*, total RNA was extracted from whole plants grown for 5, 11, 18, and 24 days, as well as dissected tissues such as; roots, young flowers, mature flowers and siliques. Using these samples, RT-PCR experiments were conducted using *AtST10* specific primers. Figure 3.1 shows the expression pattern of the gene, which is consistent with the microarray data found on Genevestigator, showing that indeed the expression of *AtST10* reaches its highest level in siliques with no detectable expression in the flowers.

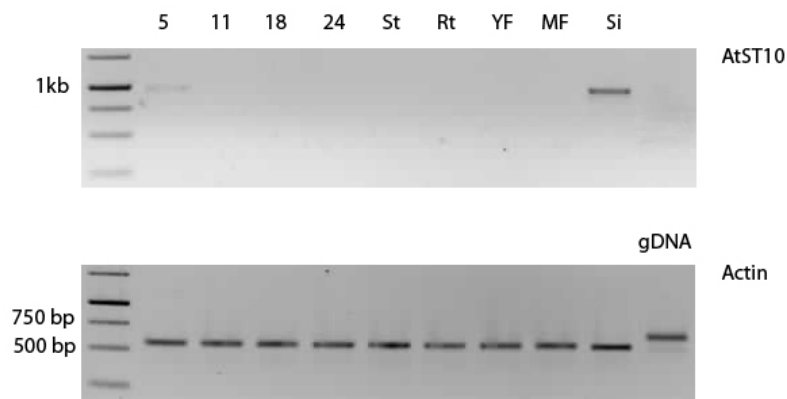


Figure 3.1. Expression level of *AtST10* at different stages of development. RT-PCR from rosettes of 5, 11, 18 and 24 day old wild-type plants; inflorescence stem (St); roots (Rt); young flowers (YF); mature flowers (MF) and siliques (Si). Actin was used as a positive control (bottom) and genomic DNA was amplified with the same actin primers to check for DNA contamination, yielding bands of 550 bp (cDNA) and ~600 bp (genomic), respectively. Molecular markers: Generuler 1kb DNA ladder (Fermentas, Lithuania). 30 cycles for *AtST10*, 25 cycles for Actin.

Genevestigator also suggests that *AtST10* is overexpressed in a *SERRATE* mutant (*se-1*). The *SERRATE* gene product is involved in the maturation of several micro RNA's. Therefore it was hypothesized that *AtST10* might be regulated either directly or indirectly by an endogenous miRNA. To test this hypothesis, computational prediction software (Adai *et al.*, 2005; <http://sundarlab.ucdavis.edu/mirna/>) was used to search for a putative micro RNA sequence that would target the *AtST10* transcript, and came across the sequence UUGGAUCAGUUGAGGAGAGC located in the mRNA of the gene At5g34867, which has a complementary sequence and would produce a stem loop pre-miRNA. RT-PCR experiments were carried out using different plant tissues to see if the putative microRNA is processed from the mRNA of gene At5g34867. The results show that when using MIR159 as a control, it showed an expected band size of 60 bp; however, no the primers used for the search of the endogenous miRNA did not produce a product (Figure 3.2)

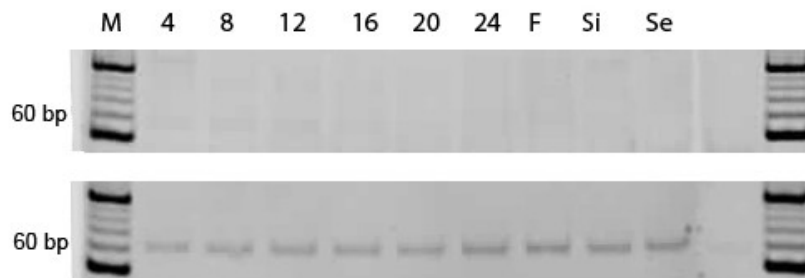


Figure 3.2. RT-PCR of putative endogenous miRNA targeting the *AtST10* transcript. The positive control, MIR159 (bottom), showed a product of roughly 60 base pairs after amplification. In contrast, the putative endogenous miRNA (top) was not amplified. From left to right: 4, 8, 12, 16, 20 and 24 day old plants, flowers (F), siliques (Si) and seeds (Se). Molecular markers (M): O'Range ruler 10 bp DNA ladder (Fermentas, Lithuania).

3.2 Molecular cloning

For the purpose of this study, we cloned the coding region of *AtST10* into two expression vectors: pRD525 and pQE30. The first one is a binary plasmid developed to overexpress a gene of interest in plants and is regulated by a doubled 35S promoter from cauliflower mosaic virus (CaMV) and the alfalfa mosaic virus (AMV) 5'UTR translational enhancer. The second is an *E. coli* expression vector with a 6x Histidine N-terminal tag developed by Qiagen (U.S.A). Due to the lack of introns in the gene, amplification was carried out directly from genomic DNA. Also, an artificial micro RNA was generated to target specifically the *AtST10* transcript for silencing. This clone was engineered by overlapping PCR using the backbone of MIR319a as a template.

3.2.1 *AtST10* overexpression

Restriction enzyme digestion showed a fragment of roughly 1 kb when the plasmid was digested with *XbaI* and *BamHI* and another of approximately 1.3 kb when the plasmid was digested only with *HindIII*, thus demonstrating that the gene was successfully cloned into pRD525. DNA sequencing results demonstrated that no errors were introduced in the sequence during amplification. Figure 3.3 shows the restriction map of the construct with the location of the regulatory elements and of the coding sequence.



Figure 3.3. Construct of transgenic *AtST10* overexpressing lines. *AtST10* coding sequence was cloned in pRD525 under the control of a doubled 35S promoter and AMV. H: *HindIII*, Bg: *BglIII*, X: *XbaI*, Ba: *BamHI*, E: *EcoRI*.

Once the proper clone was found, it was transformed into *Arabidopsis* plants. PCR amplification using a forward primer that hybridizes to the vector sequence and a reverse primer that hybridizes to the *AtST10* coding region showed the expected product of approximately 1 Kb, which was also present when using the putative transgenic plant DNA as template, and absent when using genomic DNA of a wild-type plant (Figure 3.4). This confirmed the successful insertion of the construct into the plants' genome.

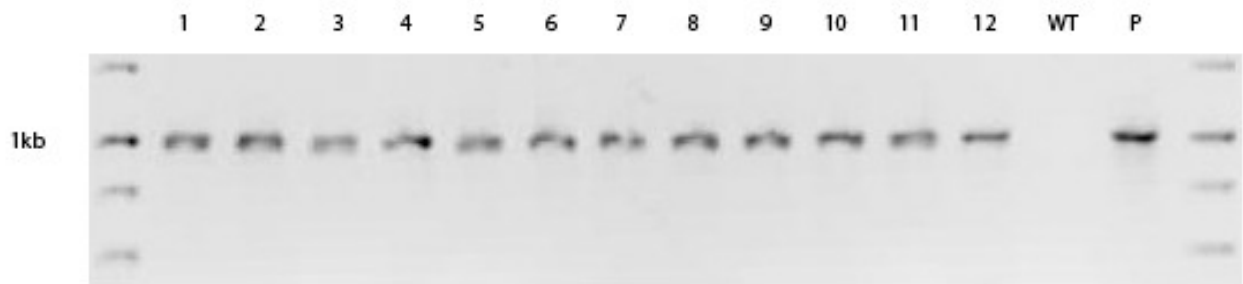


Figure 3.4. PCR amplification of *AtST10* overexpressing plants. Transgenic lines (1-12), wild-type (WT) and plasmid construct (P). Molecular markers: Gene Ruler 1kb DNA ladder (Fermentas, Lithuania).

T₁ lines were self-pollinated and the T₂ seeds from the different lines were grown on MS medium plates supplemented with 100 µg/ml kanamycin to search for lines with a single insertion. Resistance to kanamycin was the parameter used for this purpose (Table 1). Lines 2 and 4 were shown to have a single insertion of the transgene with the expected 3:1 ratio. In order to verify if the plants were overexpressing the transcript of the recombinant gene, leaf and root tissues were collected from both lines. An RT-PCR was subsequently carried out

using a forward primer that hybridizes to the AMV sequence and a reverse primer that hybridizes to the coding sequence of *AtST10*. The results show that a fragment corresponding to the expected size of the recombinant transcript is amplified in both lines (Figure 3.5).

Line	Kan ^R :Kan ^S
1	42:8
2	36:14
3	24:26
4	37:13
5	N/A
6	45:5
7	40:10
8	N/A
9	45:5
10	25:25
11	46:4
12	40:10

Table 1. Kanamycin resistance ratio of *AtST10* overexpressing plants. T₁ seeds (50) from each line were sown on MS medium supplemented with kanamycin. Resistance to the antibiotic was considered when each plant grew healthy and with a green colour. Plants were considered sensitive when the leaf tissue was white and/or the plant did not grow properly. T₁ plants from lines 5 and 8 did not grow properly, and did not produce siliques.

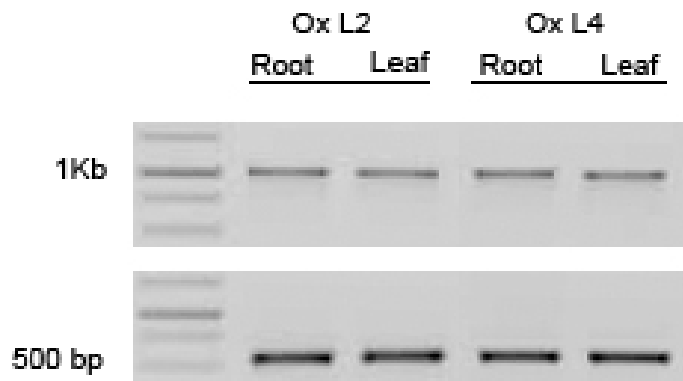


Figure 3.5. RT-PCR amplification of *AtST10* overexpressing plants. Root and leaf tissue from transgenic lines 2 and 4. Top: *AtST10* transcript. Bottom: Actin transcript. Molecular markers: Gene Ruler 1kb DNA ladder (Fermentas, Lithuania).

3.2.2 Expression of an artificial microRNA in transgenic *A. thaliana*

Due to the lack of a T-DNA insertion knockout in the coding region of *AtST10*, an artificial microRNA (amiR) was engineered to silence the expression of the gene (Figure 3.6). As described previously, the amiR was designed using web-based software. The program gave a total of 37 sequences that could be used as potential artificial miRNAs, but only one was selected among all. The selection criteria were defined by the guidelines provided on the website, specifically: 1) no mismatches between positions 2 and 12 of the amiR, 2) one or two mismatches in the 3' end of the amiR, and 3) an absolute hybridization energy between -35 and -38 kcal/mol. The artificial microRNA generated for this purpose was named *35S-35S::amiR-ST10*. Figure 3.6 shows a diagram of the construct of *35S-35S::amiR-ST10* and its restriction sites. The artificial microRNA sequence was cloned in pRD525.



```

1  AUGGAGUGAGA CCAAGAUGCC AAAGAAACUG CAAAGCGAUG ACGAAGAAAA CAUAAGUUUG
61  AUUUCUUCAC UUCCCUUUGA CGUAGAUUUC GACAGCACGA AGCUCUUCAA AUACCAAGGA
121 UGUUGGUACG ACGACAAAAC UCUGCAAGGA GUCCUCAAUU UUCAAGAGAG UUUCGAGCCA
181 CAAGACACCG AUAUAAUUU AUUCUUCGUUC CCCAAAUCUG GCACUACUUG GCUCAAAAGCU
241 CUCACGGUAG CUCUCCUGA GAGAUCCAAA CAGAAACACU CUUCUGAUGA UCAUCCUCUU
301 CUACUUGAUA AUCCUCAUGG ACUGGUACCA UUCCUCGAGC UCAGGCUGUU CACUGAGACC
361 UCGAAACCAG AUCUGACCAG UAUCUCAUCG UCGCCGAGGU UAUUUUCGAC UCAUGUGGCG
421 UUCCAAACGC UGCGAGAGGC UCUCAAAAAC UCUCCUUGUA AGAUCGUUUA CGUGUGGAGG
      UC CGCAUGACCA CAGCAAAU
481 AACGUGAAAG ACGUACUGGU GUCGUUUUGG UAUUUCACA GCGCAAAACU AAAGAUAGAA
541 GAGGAGAGAA GCAUUUUGGA UUCAUGUUC GAGUCCUUUU GCAGAGGAGU UAUCAAUUAC
601 GGACCAUCCU GGAACAUGU CUUGAACUUA UGGAGAGCAA GCUUGGAAGA CUCCAAGAAU
661 GUGCUUUUCU UGAAGUACGA GGAGUUAAAA ACAGAACCUC GCGUGCAGCU GAAGAGACUU
721 GCCGAGUUCU UGGAUUGUCC UUUUACGGUG GAAGAAGAAG AGAGGGGUAUC AGUGGAAGAG
781 AUCUUGGACC UUUGCUCAUU GCGUAACUUG AAGAAUUUGG AGAUCACAA GACCGGAAAA
841 ACGCUUAGGG GGGCCGAUCA CAAGAUUUUU UUUCGUAAAAG GGAAGUCGG UGACUCGAAG
901 AAUCAUCUGA CUCCUGAAAU GGAGAAGUA AUUGACAUGA UCACUGAGGA GAAAUUUGAA
961 GGUUCGGAUU UGAAAUUCUG A

```

Figure 3.6. Top: Construct of 35S-35S::amiR-ST10. The white square in amiR-ST10 (light grey) represents the coordinates of the mature miRNA sequence and the black square represents its complementary sequence. It is also under the control of a double 35S promoter (35S-35S) and has a terminator sequence (NOS-Ter) H: *HindIII*, Bg: *BglIII*, Ba: *BamHI*, E: *EcoRI*. **Bottom: Artificial micro RNA hybridization region.** The artificial micro RNA hybridizes to nucleotides 489-509 of the *AtST10* mRNA.

PCR amplification was performed to verify the insertion of the artificial miRNA-coding gene with primers (A and II) that were used for the construction of the recombinant gene. A fragment of the expected size (250 bp) was observed when genomic DNA of the putative transgenic line 1 was used as template. The same fragment was observed with the recombinant plasmid as template. However, no PCR product was obtained from genomic DNA of a wild type plant (Figure 3.7). This result ensured that the transgenic line had in fact at least one copy of the 35S-35S::amiR-ST10 inserted into its genome.

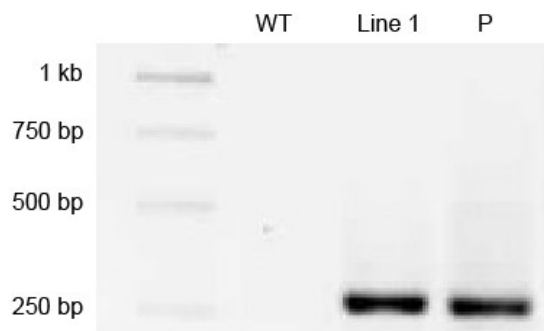


Figure 3.7. PCR amplification of artificial miRNA. Genomic DNA was extracted from a wild-type (WT) and the 35S-35S::amiR-ST10 line 1. Plasmid DNA harbouring the construct was used as a positive control. Molecular markers: Generuler 1kb DNA ladder (Fermentas, Lithuania).

RT-PCR results from wild type *Arabidopsis* and the 35S-35S::amiR-ST10 line showed that the micro RNA was being transcribed (A), and processed to the expected 60 bp product (Figure 3.8A). The observable band in the far right side of Figure 3.8A is a primer dimer, since no template was used in this lane. We also tested the impact of the microRNA on *AtST10* expression by RT-PCR. Figure 3.8B shows that the transcript of *AtST10* could no longer be detected in the amiR-ST10 line in siliques tissue.

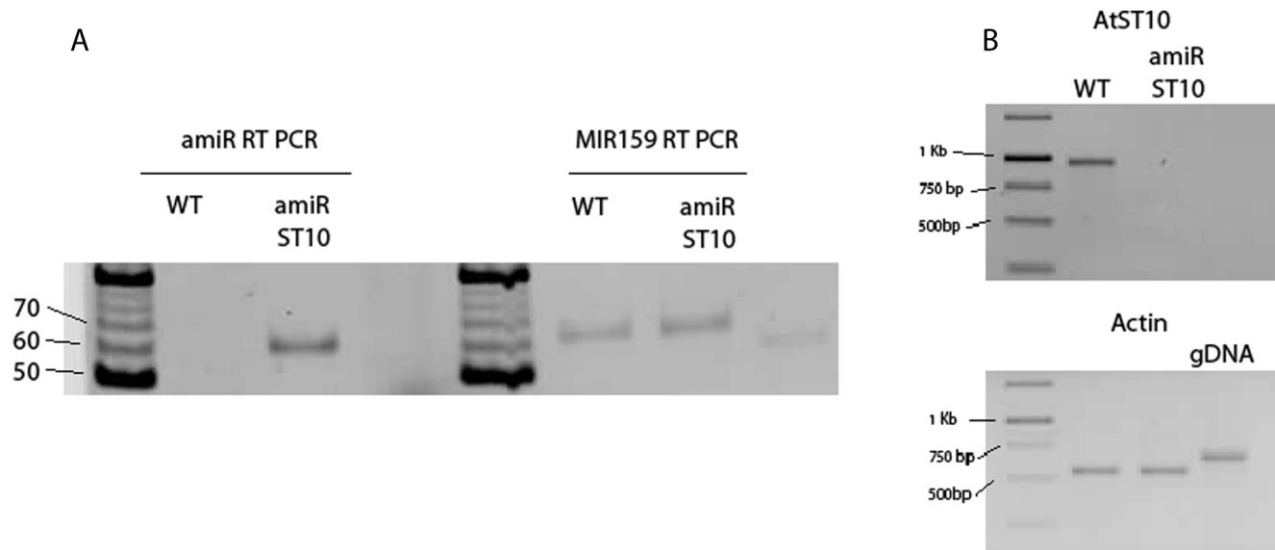


Figure 3.8. Artificial miRNA expression and function. A) RT-PCR of 35S-35S::amiR-ST10 (left) from leaf tissue with MIR159 as a positive control (right); markers: O' Range ruler 10 bp DNA ladder (Fermentas, Lithuania). B) RT-PCR of AtST10 from silique tissue (top) with actin as a positive control (bottom) and genomic DNA to detect sample contamination. Genomic DNA was used only with actin primers to detect possible contamination of DNA in the RNA samples. Markers: Gene Ruler 1kb DNA ladder (Fermentas, Lithuania). Wild-type (WT), amiR ST10 (35S-35S::amiR-ST10).

3.2.3 Cloning of *AtST10* into pQE30

As expected, digestion of the *AtST10* cDNA cloned in pQE30 with the restriction enzymes *Bam*HI and *Sph*I resulted in a fragment of approximately 1 kb, whereas digestion with *Hind*III resulted in a smaller fragment (379 kb). Sequencing results confirmed that no errors were introduced in the sequence during amplification and an amino acid alignment showed an identical sequence, except for the histidine tag located in the N-terminus of the recombinant protein. Figure 3.9 shows the elements of the construct as well as the mentioned restriction sites.



Figure 3.9. Construction of *AtST10* in pQE30. The coding sequence of *AtST10* was cloned into pQE30, a plasmid that contains the regulatory elements of the lac operon and a 6x histidine tag upstream of the multiple cloning sites. B: *Bam*HI, H: *Hind*III, S: *Sph*I.

3.3 Biochemical characterization of *AtST10*

To identify the substrate and product of *AtST10*, plant metabolites were extracted from siliques of ~45 day old *Arabidopsis* plants. We used ³⁵S-radiolabeled PAPS as sulphonate donor to assay the activity of the recombinant enzyme with the plant extracts. To demonstrate the *in vivo* accumulation of the possible reaction products, we used thin layer chromatography, reverse phase high performance liquid chromatography and neutral loss mass spectrometry. Also, the metabolite profiles of wild-type, overexpressor and artificial micro RNA lines were compared using neutral loss mass spectrometry, liquid chromatography mass spectrometry (LC-MS) and tandem mass spectrometry (MS/MS).

3.3.1 Expression of recombinant AtST10 sulfotransferase

In order to determine the biochemical function of AtST10, the coding sequence was cloned into the *E. coli* expression vector described above and the histidine tag was used for affinity purification on a Ni-NTA agarose column. Polyacrylamide gel electrophoresis showed that a protein of approximately 40 kDa, a molecular weight that corresponds to the HisTag-AtST10 fusion (39.21 kDa), was produced after inducing the cell culture with 1 mM IPTG. Further evidence of the production of the protein was acquired when a western blot was probed with polyclonal anti-sulfotransferase antibodies, where the empty plasmid (pQE30) and the uninduced did not produce a band, but the induced and purified extracts showed a band of ~40 kDa (Figure 3.10).

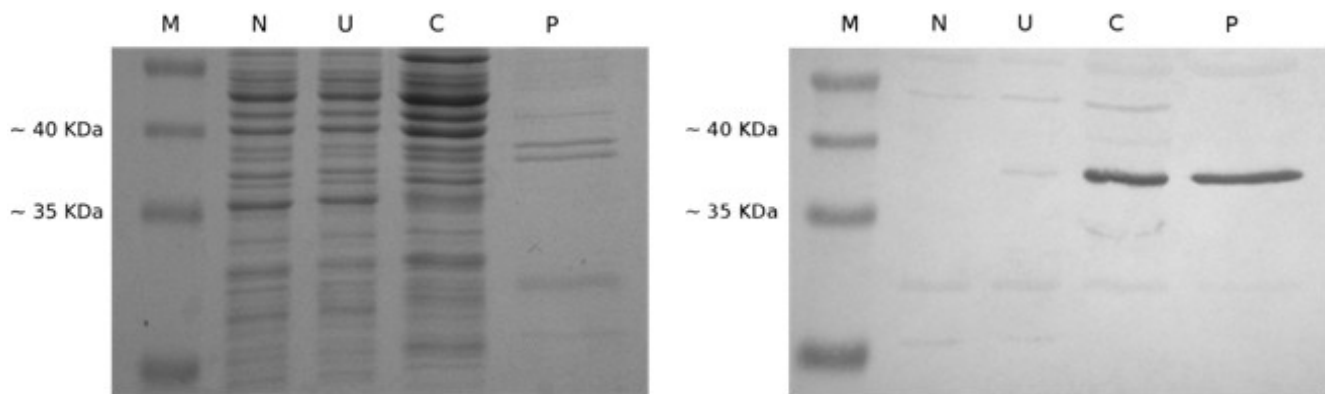


Figure 3.10. Expression of recombinant protein in *E. coli*. SDS PAGE analysis (left) showed expression of AtST10 recombinant protein, which was confirmed by Western Blot (right) using a sulfotransferase polyclonal antibody. A band of approximately 38 kDa was observed, a size that corresponds to the AtST10 protein. M: Marker; N: negative control; U: uninduced crude extract; C: induced crude extract (25 μ g); P: purified protein (5 μ g). Protein marker: PageRuler (Fermentas, Lithuania).

3.3.2 HPLC purification of AtST10 product and substrate

As shown in microarray data from the Genevestigator website, the highest level of expression of *AtST10* is in the siliques of *Arabidopsis thaliana*. Consequently, silique extracts were used to purify the potential substrate of AtST10. Also, extracts from seeds of *B. napus* were used.

3.3.3 HPLC purification of AtST10 enzymatic reaction product

To identify the product of the reaction, an enzyme assay was performed using an *Arabidopsis* silique extract and the recombinant protein expressed in *E. coli*. Following the assay, the radiolabeled-sulfated product was purified by reverse phase HPLC and was found to elute in fractions 27 and 28 (Figure 3.11).

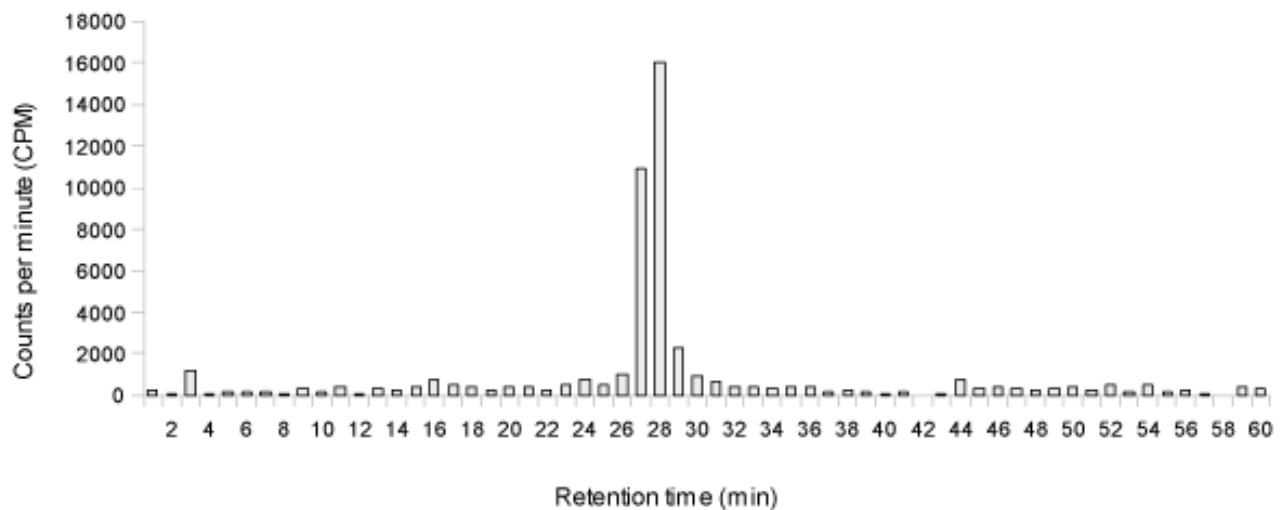


Figure 3.11. HPLC purification of radiolabeled enzymatic product. The enzymatic product elutes in fractions 27 and 28.

3.3.4 Thin layer chromatography of the AtST10 enzymatic product

Approximately 10,000 CPM of the *in vitro* enzymatic reaction product with metabolites from *A. thaliana* siliques and *B. napus* seeds were spotted on a cellulose TLC plate and separated using a n-butanol-acetic acid-water solvent (6:2:2, v/v/v) (Figure 3.12). The results show that the products of the two reactions might be the same since they migrate at the same relative distance compared to the solvent front.

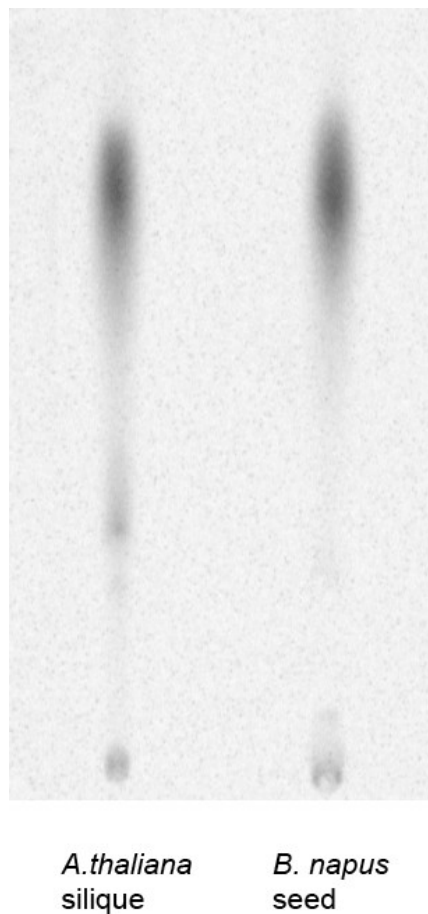


Figure 3.12. TLC plate of recombinant AtST10 *in vitro* reaction products. *Arabidopsis thaliana* and *Brassica napus* extracts were used as substrates. The TLC sample migration was performed with n-butanol-acetic acid-water (6:2:2; v/v/v).

To purify the reaction product, the *in vitro*-labelled enzymatic products were co-chromatographed along with a crude metabolite extract. The TLC band corresponding to the AtST10 product from *Arabidopsis thaliana* and *Brassica napus* extracts was excised and

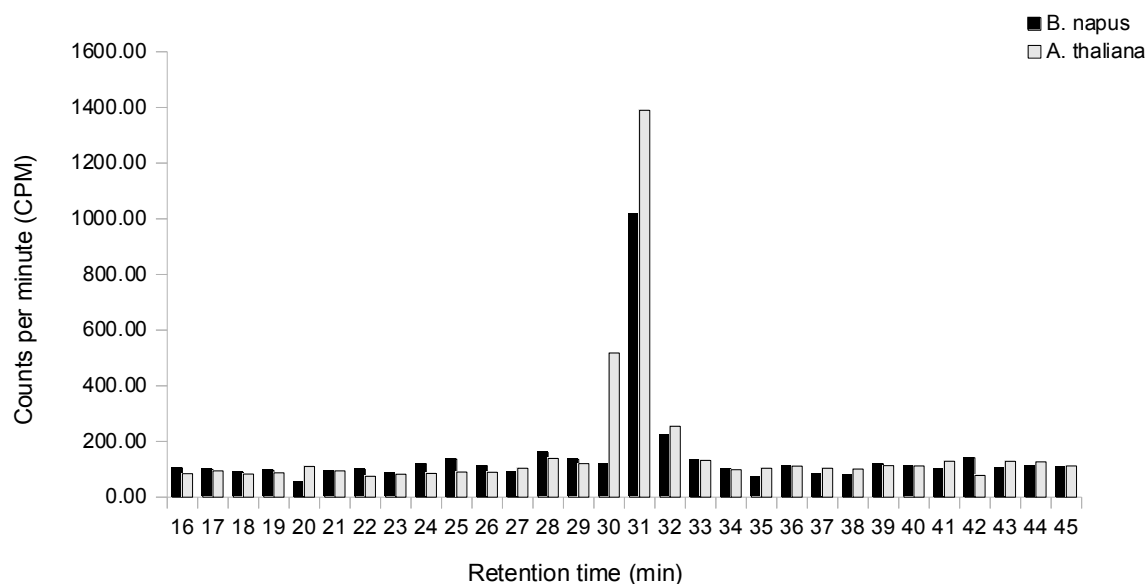


Figure 3.13. HPLC profile of hydrolyzed TLC spots from *Arabidopsis* siliques and *Brassica* seeds extracts.

extracted in 50:50 methanol:water and subsequently treated by mild hydrolysis to remove the sulphonate group. The TLC-purified hydrolyzed metabolites were later fractionated using reverse phase high performance liquid chromatography (HPLC) and the fractions were assayed using the AtST10 recombinant enzyme. The result showed that in both cases the highest enzymatic activity was obtained with fraction 31 (Figure 3.13).

3.3.5 Mass spectrometry

To elucidate the structure of the substrate and product, we carried out LC-MS using the neutral loss function. The neutral loss function allows the identification of only the molecules that lose a mass of 80 Da corresponding to the sulphonate anion upon fragmentation. We

could also compare the spectra from total extracts from siliques of wild type and of the transgenic lines (Figure 3.14).

The LC-MS spectra contain multiple putative sulphonated compounds and no clear differences were observed between the wild type, overexpressing and artificial miRNA silique extracts. To identify the AtST10 enzymatic product we opted for the purification of the sulphonated metabolites from a TLC plate. Regions of the *Arabidopsis* and *Brassica* metabolite extracts which were migrating at the same level as the AtST10 radiolabeled product were excised and extracted in 50:50 methanol:water with 5 mM ammonium acetate and subsequently analysed by neutral loss mass spectrometry (neutral loss of 80 Da). The TLC bands of both non-hydrolysed *Arabidopsis* and *Brassica* extracts showed that the molecule with the highest abundance had a mass of 307.2 Da [M+H] (Figure 3.15). A molecule with a mass of 305.2 Da [M+H] was also present in the TLC-purified fraction. This molecule gave the same fragmentation pattern as 12-hydroxyjasmonate sulphate, which was previously shown to be the reaction product of AtST2a. To test the possibility that 12-hydroxyjasmonate sulphate is also the reaction product of AtST10, an enzyme assay was carried out using recombinant AtST10 and authentic 12-hydroxyjasmonate as substrate; however, no activity could be detected when 12-hydroxyjasmonate was used as substrate (Figure 3.16).

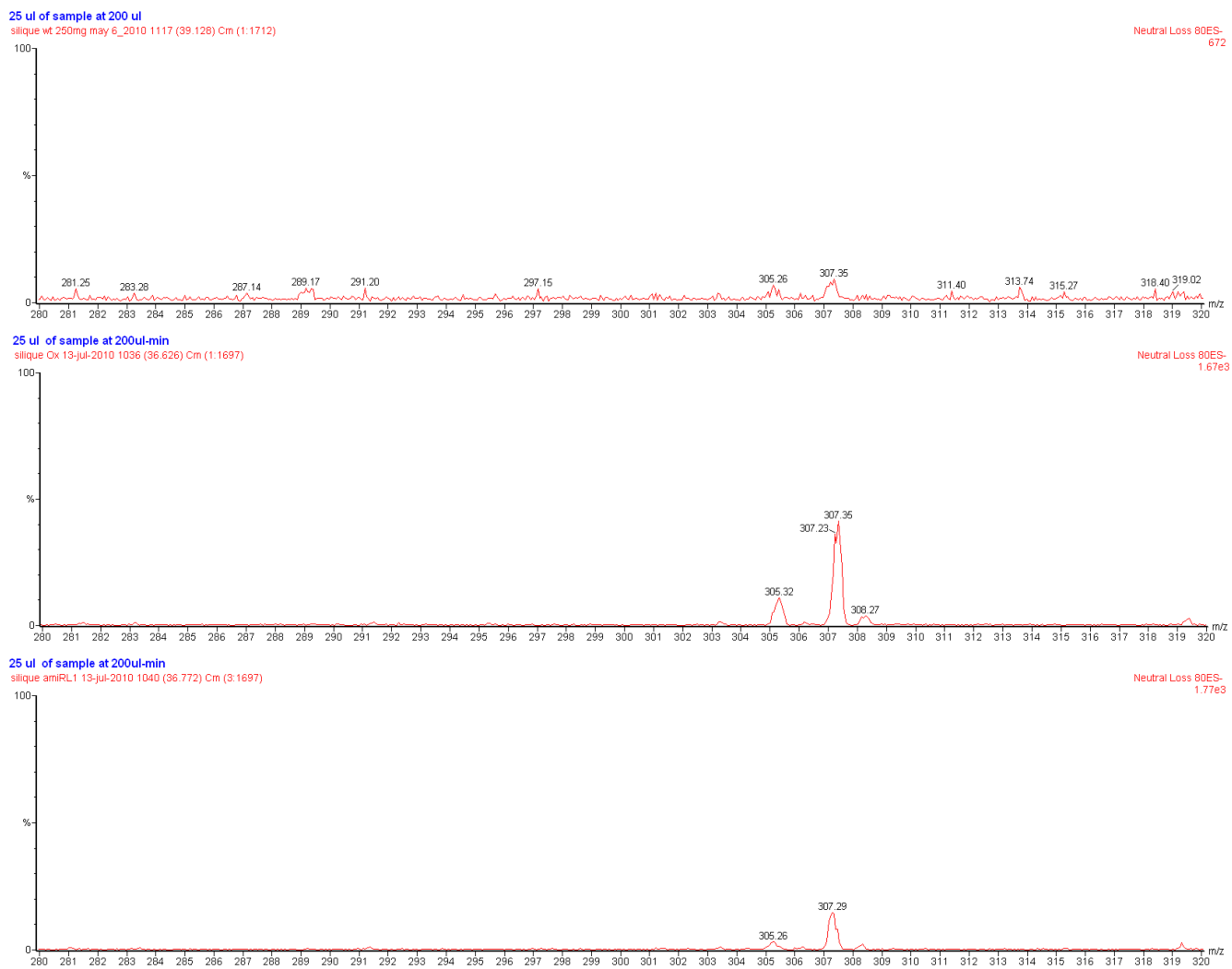


Figure 3.14. Mass spectra of silique extracts from wild-type and transgenic lines. Top: wild-type siliques. Center: AtST10 overexpressor line. Bottom: artificial micro RNA line.

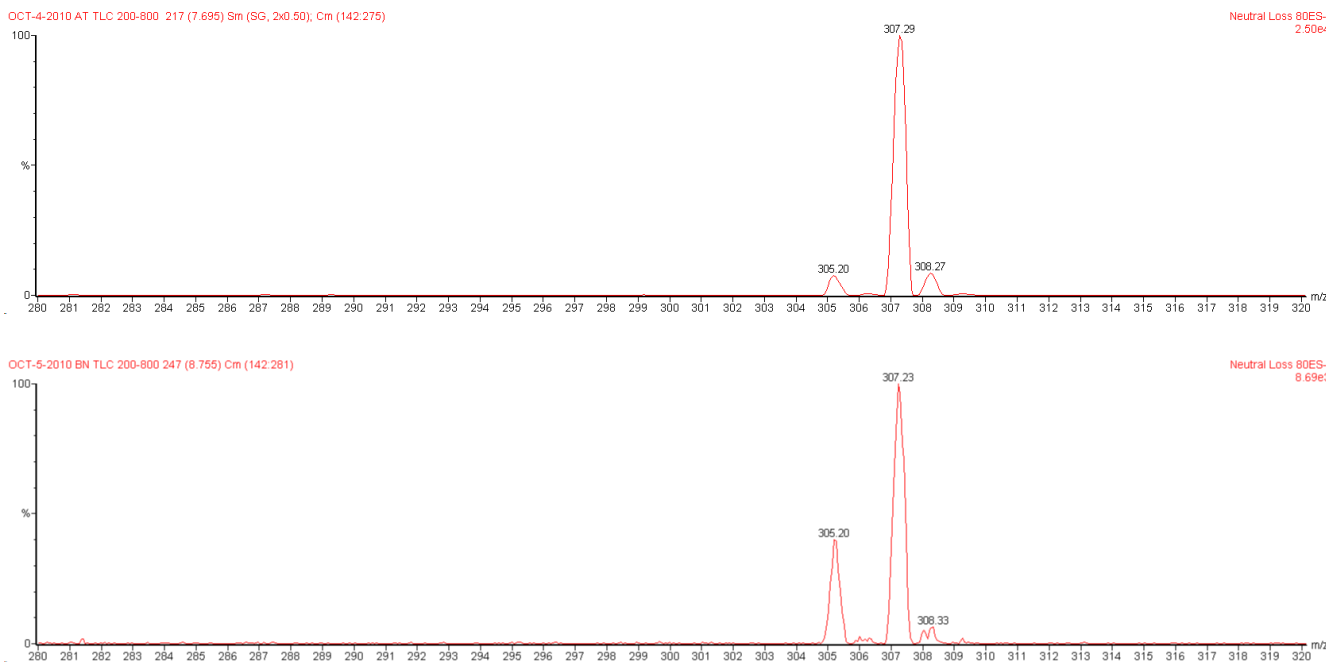


Figure 3.15. Mass spectra of *Arabidopsis* and *Brassica* compounds purified from TLC plates.

Extracts from *Arabidopsis* siliques (top) and *Brassica* seeds (bottom) were purified by TLC and later analyzed by neutral loss mass spectrometry. A mass of 307.2 Da [M+H] was observed in both extracts, suggesting it to be the potential product of AtST10 sulfotransferase. The second prominent peak is 305.2 [M+H] and corresponds to a previously identified compound 12-hydroxyjasmonate sulfate.

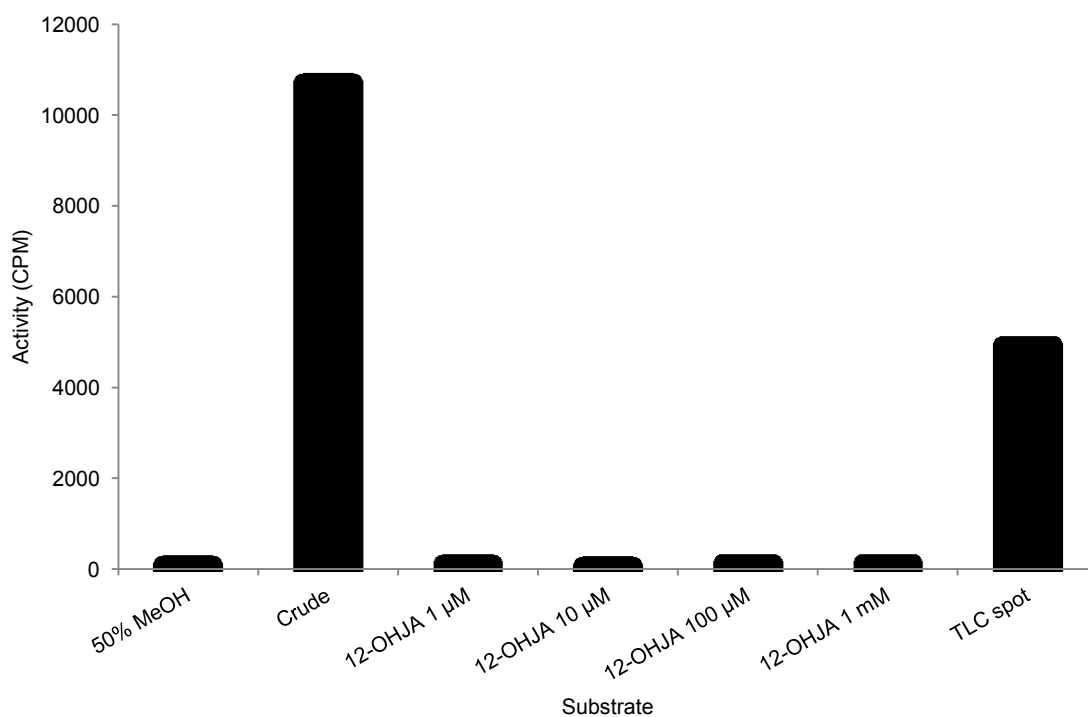


Figure 3.16. Activity of AtST10 using 12-hydroxyjasmonate as substrate. The recombinant enzyme was assayed using 12-hydroxyjasmonate as substrate. Activity was detectable only in a crude plant extract and a hydrolyzed TLC band.

In order to see if the molecules with a mass of 305 and 307 Da are present in other parts of the plant, we repeated the TLC purification procedure with non-hydrolysed extracts from seedlings, roots and rosettes. Neutral loss mass spectrometry of the TLC-purified spots showed that the molecules previously found in the siliques and the seeds, were not detected or present in very small quantities in roots, rosette leaves and seedlings (Figure 3.17).

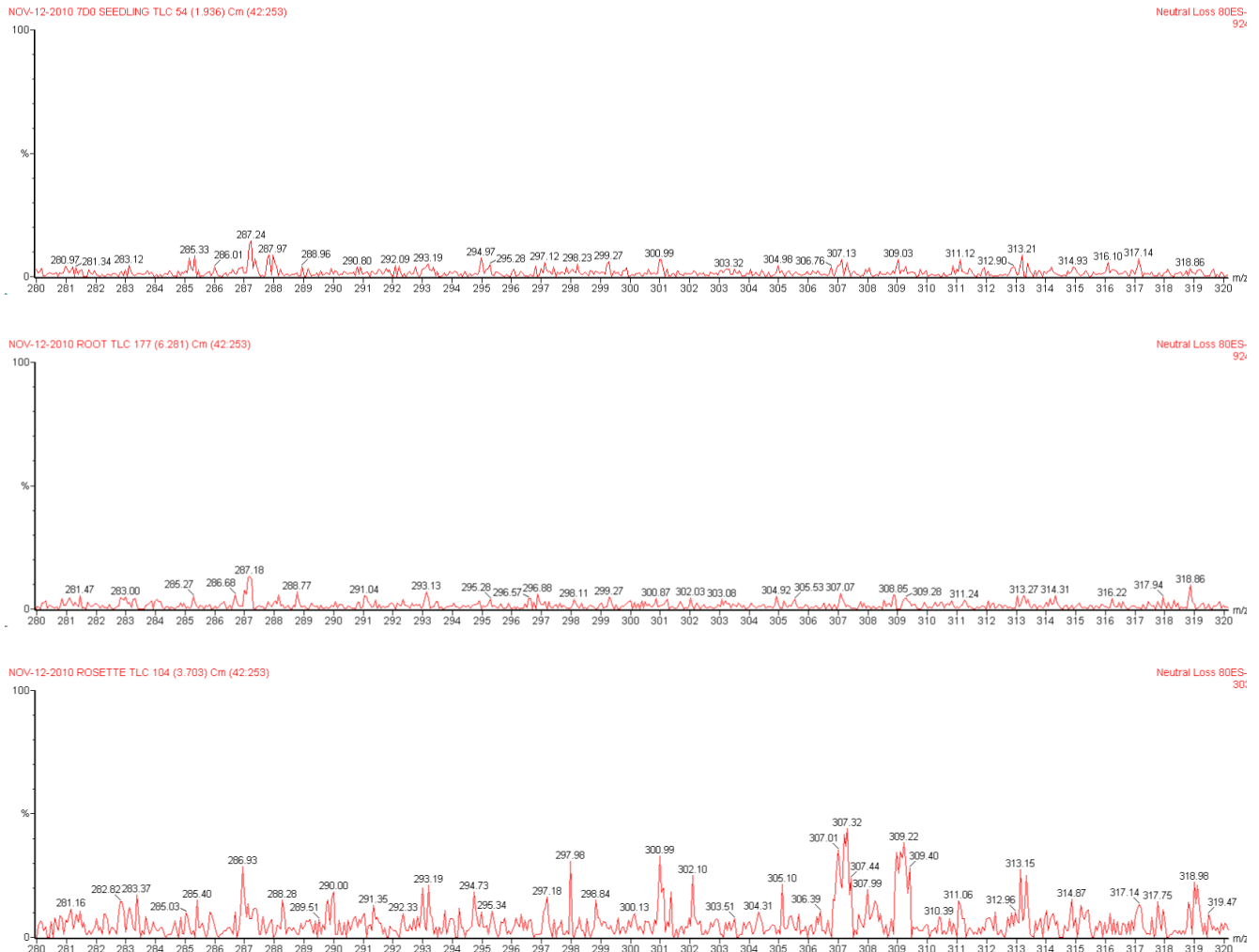


Figure 3.17. Mass spectra of compounds from various tissues purified from TLC scrapes. Extracts from wild-type *Arabidopsis* 7 day old seedlings (top), roots (center) and rosette leaves (bottom) were purified by TLC and subsequently analyzed by neutral loss mass spectrometry. The masses previously found in siliques and seeds are present in very small quantities in the three mass spectra.

The same procedure of purification by TLC and analysis by neutral loss mass spectrometry was carried out for the transgenic lines. The results, presented in Figure 3.18, show that the molecule with a molecular mass of 307 Da is also predominant in the overexpressor line, but is also present in the artificial micro RNA line. However, the compound with a m/z of 305 [M+H] seemed to be the most affected in the amiR line. Table 2 shows the relative abundance of both the 305 and 307 molecular ions in the different genotypes.

Mass	Genotype		
	Wild-type	Overexpressor	35S-35S::amiR-ST10
305	7.41x10 ⁴	3.28x10 ⁴	1.42x10 ⁴
307	3.35x10 ⁵	3.48x10 ⁵	6.40x10 ⁴

Table 2. Relative abundance of the 305 and 307 ions in wild-type, overexpressor and artificial miRNA lines

Tandem mass spectrometry (MS/MS) of plant extracts (Figure 3.19) showed that the molecule with a molecular mass of 307 Da is indeed a sulphated compound, since the fragmentation pattern shows a fragment of 96.97 Da, a mass which corresponds to HSO₄⁻. Other significant fragments were found and will be discussed later.

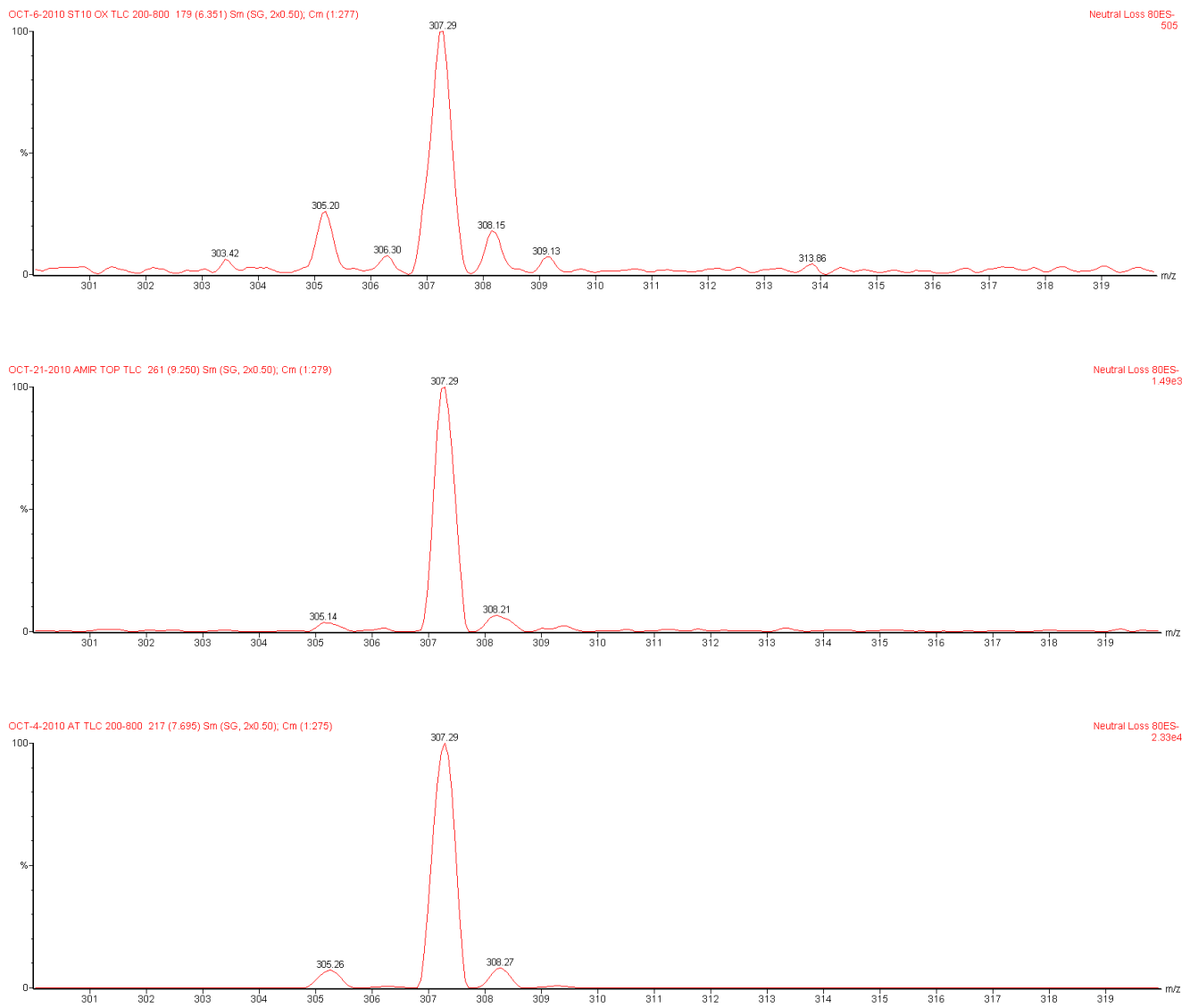


Figure 3.18. Neutral loss mass spectrometry of TLC-purified compounds from wild-type and transgenic lines. Top: Overexpressor line; center: Artificial micro RNA line; bottom: wild type.

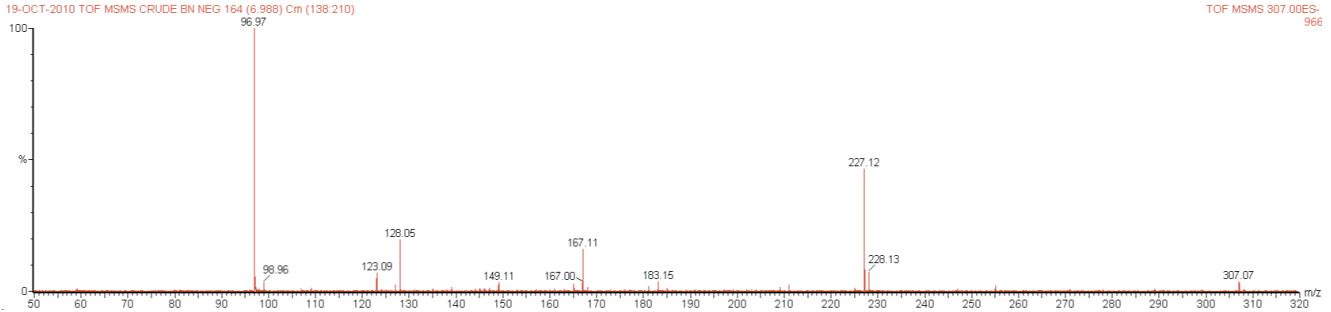


Figure 3.19. Fragmentation pattern of the m/z 307 [M+H] molecular ion. The TLC purified metabolite was fragmented using a collision energy of 30 eV.

3.4 Morphometric analyses of the transgenic lines

As mentioned earlier, the expression of *AtST10* reaches its highest level in siliques of wild-type plants. To investigate the role of *AtST10* in the development of the plant, we analysed the development of the seeds and siliques. A total of thirty siliques were collected from the wild-type, overexpressor and artificial micro RNA lines, and the seeds of each individual silique of each group were counted. The length and width of approximately one hundred seeds from each line was also measured in order to calculate the seed volume by using the formula: $\frac{4}{3} \cdot \pi \cdot \text{length} \cdot \text{width} \cdot \text{depth}$ (Riefler et al., 2006), where the depth was considered to be the same as the width.

Figure 3.20 shows the seed production among the genotypes. On average, seed production per silique was 44.9 (SD ± 6.64), 44.2 (SD ± 9.04), 29.3 (SD ± 3.69) and 35 (SD ± 5.03) for the wild-type (WT), amiR, OxL4 and OxL2 lines, respectively. Tukey's Honestly Significant Difference (HSD) test shows that there is no significant difference between WT and amiR, but

that the mean of WT is different from OxL4 and OxL2 ($P < .01$). Seed production of the amiR line was also significantly different from both overexpressor lines ($P < .01$). The number of seeds among both overexpressor lines was also significantly different ($P < .01$).

Figure 3.21 shows seed volumes from the different lines. Tukey's HSD test shows that seed volume of wild-type plants ($116.4 \mu\text{m}^3 \pm 29.96$) are significantly different from the volume of both overexpressor lines (L4: $187.6 \mu\text{m}^3 \pm 22.19$; L2: $165.2 \mu\text{m}^3 \pm 27.29$) and the artificial miRNA line ($151.4 \mu\text{m}^3 \pm 21.70$) with a $P < .01$. Comparison of the mean of the amiR line versus that of the OxL4 and OxL2 lines also shows a difference ($P < .01$). However, there is no significant difference between the seeds of the overexpressor lines ($P < .01$).

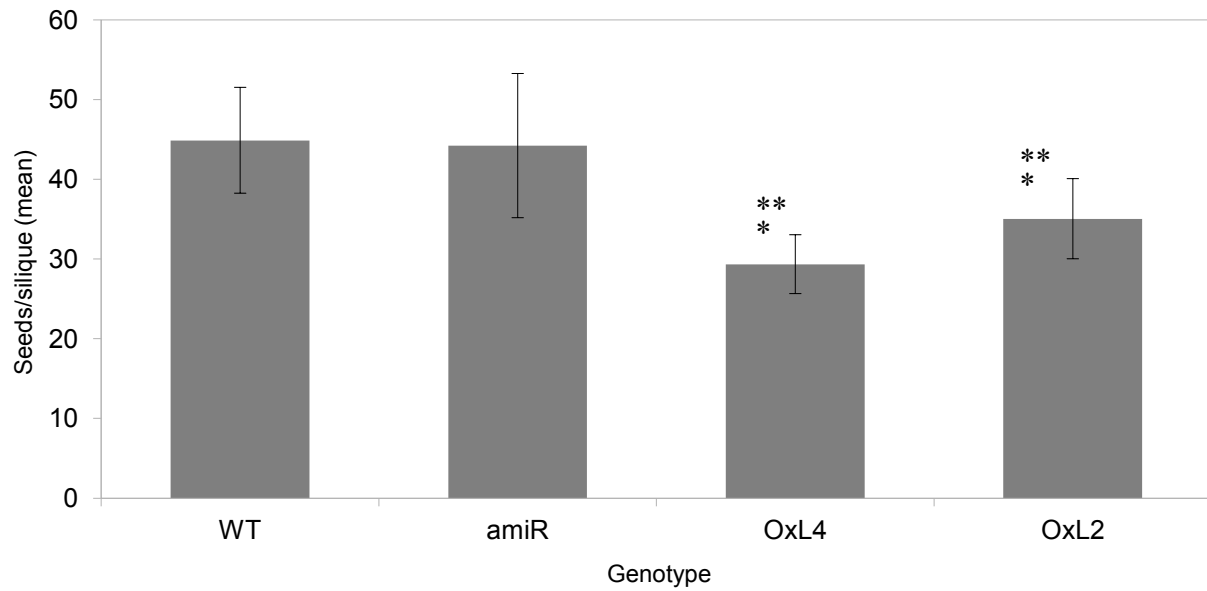


Figure 3.20. Seed production of wild-type and *AtST10* transgenic lines. Mean value of seeds per silique of wild-type (WT) 35S-35S::amiR-ST10 (amiR) *AtST10* overexpressor lines OxL4 and OxL2.

*Significantly different from WT ($P < .01$); ** significantly different from amiR ($P < .01$).

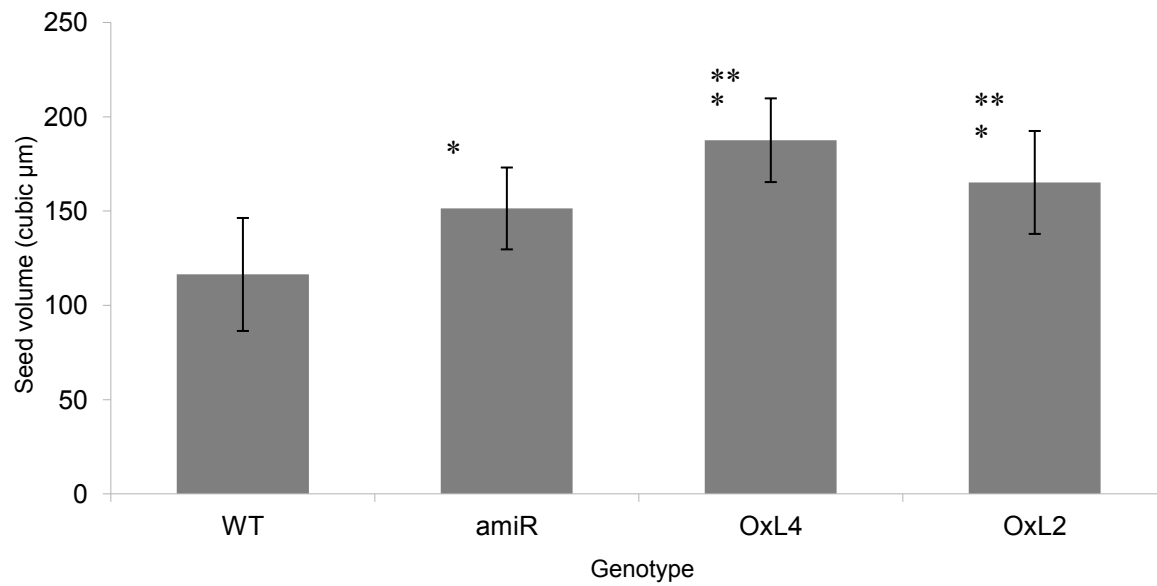


Figure 3.21. Seed volume (μm^3) of wild-type (WT), 35S-35S::amiR-ST10 (amiR) and AtST10 overexpressor lines OxL4 and OxL2. *Significantly different from WT ($P < .01$); ** significantly different from amiR ($P < .01$).

4. Discussion

Analyses of publicly available microarray data (Genevestigator) showed that *AtST10* has its highest level of expression in siliques (Zimmermann *et al.*, 2004). This result was confirmed by transcript expression analysis of several plant parts at different stages of development of *Arabidopsis*, where, in fact, an amplified *AtST10* transcript was observable in RNA samples from siliques, whilst the level of expression was lower or below the levels of detection in other tissues (Figure 3.1). This result suggests that this sulfotransferase might play a role in seed development.

As mentioned in chapter one, *SERRATE* is a zinc finger protein involved in the maturation process of miRNAs (Lobbes *et al.*, 2006). Analysis of the microarray data showed that a mutation in the *SERRATE* gene causes an up-regulation of *AtST10* (Genevestigator). This gave an insight into the possibility of *AtST10* expression being under the control of a miRNA. We searched for putative miRNA sequences targeting *AtST10* directly by using the web-based computational prediction software developed by Adai *et al.* (2005). The search revealed the sequence 5'-UUGGAUCAGUUGAGGAGAGC-3' as a possible candidate, located in *At5g34867* and targeting the *AtST10* transcript from nucleotides 249 to 269. However, RT-PCR results from several tissues did not show amplification of this sequence (Figure 3.2), suggesting that this is not present as miRNA sequence in the plant. Nevertheless, the possibility of *AtST10* being regulated by miRNA was not discarded due to the strong evidence provided by microarray analyses. It is possible that the negative effect of *SERRATE* on *AtST10* expression is indirect and does not involve miRNA targeting its transcript but the transcript of another gene that positively regulates *AtST10* expression.

Given that the expression of *AtST10* is detectable almost exclusively in siliques, special attention was given to seed phenotype in overexpressor lines. We looked specifically for a change in seed number and/or morphology. Statistical analyses of the data showed that plants overexpressing *AtST10* produce fewer seeds than the wild-type and *35s-35s::amiR-ST10* genotypes (Figure 3.20). However, the seeds of the overexpressor lines are bigger than their equivalent in wild type plants (Figure 3.21), suggesting a role for *AtST10* in seed and/or embryo development. In support of this hypothesis, it is interesting to note that the *Arabidopsis lec1-1* (*LEC1* leafy cotyledon 1 mutant) has a higher expression of *AtST10* (Genevestigator). *LEC1* is a transcription factor required for proper embryogenesis in *A. thaliana* (Braybrook and Harada, 2008). However, in view of the relatively mild phenotype of the *AtST10* overexpressor lines, its role in embryonic development must be minor and still needs to be characterized.

The strict tissue localization of *AtST10* expression and the abnormal seed development of the overexpressor lines prompted us to identify the substrate and product of the enzyme. Neutral loss mass spectrometry of the TLC-purified product from *Arabidopsis* wild-type siliques revealed a prominent molecular ion with a mass of 307 Da [M+H] as well as a minor molecular ion with a mass of 305 Da [M+H] corresponding to the previously characterized 12-hydroxyjasmonate sulfate. The fragmentation pattern of the 307 Da molecular ion by tandem mass spectrometry confirmed that it contains a sulfonate ester with a signature ion at 96.97 Da (HSO₄⁻). Apart from the presence of the 96.97 Da ion, the fragmentation pattern was found to be similar to the one observed previously with 12-hydroxyjasmonate (Gidda, *et al.* 2006). However, for the silique-purified intact molecule and some of its fragments a difference of +2 mass units is observed (Figure 4.1). It has been shown previously that the fragmentation of 12-hydroxyjasmonate sulphate (305 Da [M+H]) releases a major fragment

with a molecular mass of 225 Da ($C_{12}H_{18}O_4$) corresponding to the de-sulfonated hydroxylated derivative of jasmonic acid. In the case of our unknown molecule, the fragment with a molecular mass of 227.12 Da [$C_{10}H_{16}O_2+H$] corresponds to the reduced form of 12-hydroxyjasmonate. This is the first report of the existence of this molecule in plants.

In addition to the hydroxylation of jasmonic acid (JA) at carbon 11 and 12 to produce 11-hydroxyjasmonate and 12-hydroxyjasmonate (Gidda *et al.* 2003), respectively, it has been reported that JA undergoes several other modifications; one of them being a reduction of carbon 6 to form cucurbitic acid (Sembder *et al.*, 1994). It is possible that there is another reductase attacking either carbon 9 or carbon 10 of 12-OHJA to form a reduced version of the molecule by eliminating the double bond between both carbon atoms. This reduction reaction would generate a novel molecule two mass units higher than 12-OHJA (Figure 4.1). In view of the high structural similarity between our unknown molecule and the previously characterized 12-hydroxyjasmonate, we tested the AtST10 recombinant enzyme with the latter compound. Interestingly, the enzyme does not accept 12-OHJA (Figure 3.16) suggesting a strict requirement for the reduced sided chain for catalysis. It is well known that jasmonic acid and its methyl ester (JA) play an important role in plant defence to pathogens and wounding (Koo and Howe, 2009). Several modification reactions of jasmonic acid such as; hydroxylation, esterification with amino acids and glycosides also generate a large number of derivatives collectively called jasmonates. Initially, these reactions were believed to be involved in the inactivation of jasmonic acid. Some recent experimental evidence suggests that some of the jasmonic acid derivatives are required for proper flower and tuber development (Wasternack, 2007). However, their specific role in these important developmental processes is still unknown.

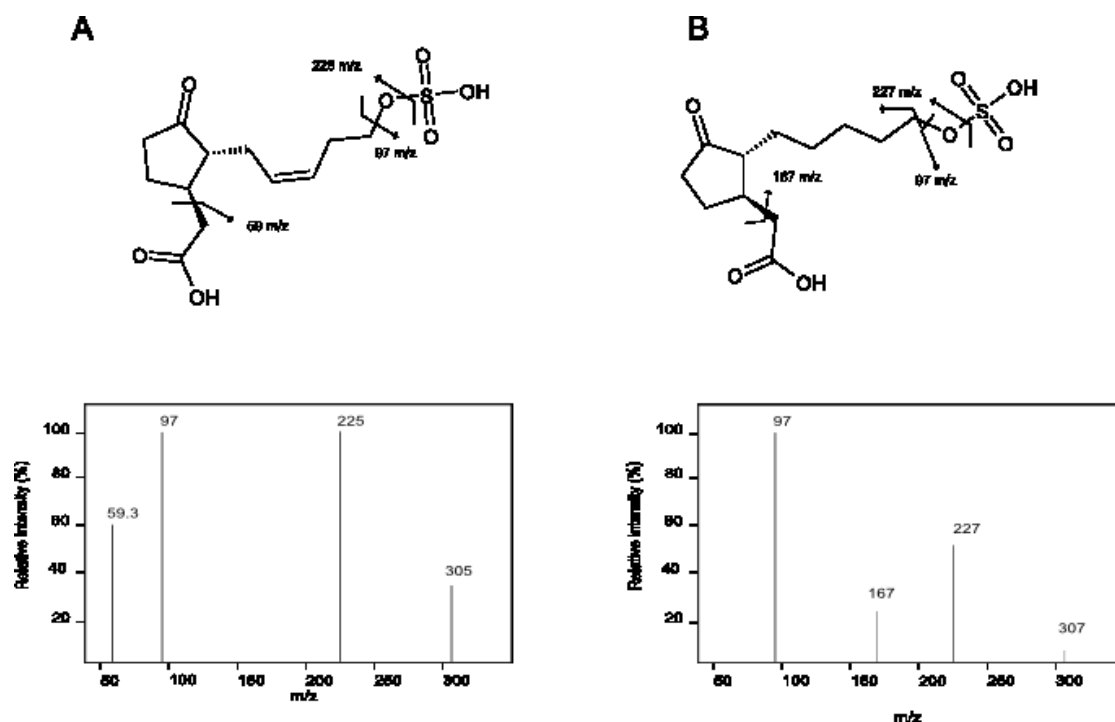


Figure 4.1. Deduced chemical structures of 12-OHJA (A) and its reduced form (B). The arrows on the structures represent the places where the bonds in molecules are broken by tandem mass spectrometry to give the fragmentation patterns as seen below each one.

Thin layer chromatography revealed that the reaction products of the recombinant AtST10 protein, using extracts from *A. thaliana* siliques and *B. napus* seeds in enzyme assays, have the same retention time on HPLC, and the same migration behaviour on TLC (Figure 3.12). This suggests that the same molecule is sulfonated in the two plants. This result is supported by the fact that neutral loss mass spectrometry of the TLC-purified reaction products shows peaks with the same mass (Figure 3.15).

Unfortunately, there is no loss of function mutant available for *AtSt10* that would allow defining without any ambiguity its biochemical and biological function *in vivo*. Even though the expression of the *35S-35S::amiR-ST10* effectively reduced the accumulation of the *AtST10*

transcript to undetectable levels (Figure 3.8), it failed to eliminate the accumulation of the 307 Da molecule (Figure 3.18). A possible reason for this could be that the real product of the AtST10-catalyzed reaction is present in minute quantities and could not be detected in our experiments. However, increasing the amount of material always produced the same mass spectra with only the 305 and 307 Da sulfonated compounds. Another possibility is that the substrate molecule is not exclusive to the AtST10 protein and that another sulfotransferase is compensating for the accumulation of the 307 Da molecular ion. Previous studies done in our laboratory have shown that it is the AtST2a protein that catalyzes the sulfonation of 12-hydroxyjasmonate ([M+1] mass = 305Da). We never tested AtST2a with the reduced form of 12-hydroxyjasmonate to see if it can act as a substrate and could compensate for the loss of function of AtST10 in the *35S-35S::amiR-ST10* lines.

Future work

More experiments will have to be performed to confirm that the reduced form of 12-hydroxyjasmonate is the *in vivo* substrate of AtST10. To reach this objective, different protocols will have to be developed to purify the substrate and product to homogeneity from large plant samples.

The overexpression of AtST10 led to a reduction in seed production suggesting that proper levels of the reduced form of 12-hydroxyjasmonate must be present for normal seed production. To confirm this hypothesis, we will have to demonstrate that there is a reduction in the accumulation of the reduced form of 12-hydroxyjasmonate in the *AtST10* overexpressor lines. It would also be interesting to see if the exogenous application of the reduced form of 12-hydroxyjasmonate can modify seed set in *Arabidopsis*.

It has been shown previously that the exogenous application of 12-hydroxyjasmonate induces the expression of a subset of genes different from the one induced by jasmonic acid. Similar experiments should be done with the reduced form of 12-hydroxyjasmonate to see if it affects the expression of genes known to be involved in seed development. Unfortunately, the reduced form of 12-hydroxyjasmonate is not available commercially and would need to be synthesized to perform some of the experiments described above.

5. References

- Adai, A., Johnson, C., Mlotshwa, S., Archer-Evans S., Manocha, V., Vance, V., and Sundaresan, V.** (2005) Computational prediction of miRNAs in *Arabidopsis thaliana*. *Genome Research*, **15**:78-91.
- Barte, D.P.** (2004) MicroRNAs: genomics, biogenesis, mechanism, and function. *Cell* 2004, **116**:281-297.
- Braybrook, S.A., and Harada, J.J.** (2008) LECs go crazy in embryo development. *Trends in plant science*, **13**:624-30
- Chapman, E.J., and Carrington, J.C.** (2007) Specialization and evolution of endogenous small RNA pathways. *Nature Review Genetic*, **8**:884-896
- Farzan, M., Mirzabekov, T., Kolchinsky, P., Wyatt, R., Cayabyab, M., Gerard, N.P., Gerard, C., Sodroski, J., and Choe, H.** (1999) Tyrosine sulfation of the amino terminus of CCR5 facilitates HIV-1 entry. *Cell*, **96**:667-676
- Gidda S.K., Varin, L.** (2006) Biochemical and molecular characterization of flavonoid 7-sulfotransferase from *Arabidopsis thaliana*. *Plant Physiology and Biochemistry* **44**:628-636
- Gidda, S.K., Miersch, O., Levitin, A., Schmidt, J., Wasternack, C., Varin, L.** (2003) Biochemical and molecular characterization of a hydroxyjasmonate sulfotransferase from *Arabidopsis thaliana*. *Journal of Biological Chemistry* **278**:17895-17900
- Gregory, B.D., O'Malley, R.C., Lister, R., Urich, M.A., Tonti-Filippini, J., Chen, H., Millar, A.H., and Ecker, J.R.** (2008) A link between RNA metabolism and silencing affecting *Arabidopsis* development. *Development Cell*, **14**:854-866.
- Hernández-Sebastiá, C., Varin, L., Marsolais, F.** (2008) Sulfotransferases from Plants, Algae and Phototrophic Bacteria, *Advances in Photosynthesis and Respiration*, Vol 27.

Springer Netherlands

Khodashenas, E. (2010) Characterization of the Function of the AtST4 Subfamily Members in Cytokinin-Dependent Growth Control in *Arabidopsis thaliana*. (Master's thesis). Concordia University, Montréal, Québec

Klein, M., and Papenbrock, J. (2004) The multi-protein family of Arabidopsis sulphotransferases and their relatives in other plant species. *Journal of Experimental Botany*, **55**:1809-1820

Klein, M., Reichelt, M., Gershenzon, J., and Papenbrock, J. (2006) The three desulfoglucosinolate sulfotransferase proteins in *Arabidopsis* have different substrate specificities and are differentially expressed. *FEBS Journal* **273**:122-136

Koo, A.J., Howe, G.A. (2009) The wound hormone jasmonate. *Phytochemistry*, **70**:1571-80.

Laubinger, S., Sachsenberg, T., Zeller, G., Busch, W., Lohmann, J.U., Ratsch, G., and Weigel, D. (2008) Dual roles of the nuclear cap-binding complex and SERRATE in pre-mRNA splicing and microRNA processing in *Arabidopsis thaliana*. *PNAS*, **105**:8795-8800.

Lobbes, D., Rallapalli, G., Schmidt, D.D, Martin, C., and Clarke, J. (2006) SERRATE: a new player on the plant microRNA scene. *European Molecular Biology Organization*, **7**:1052-1058.

Mallory, A.C., and Bouché, N. (2008) MicroRNA-directed regulation: to cleave or not to cleave. *Trends in Plant Science*, **13**:359-367.

Mallory, A.C., Elmayan, T., and Vaucheret, H. (2008) MicroRNA maturation and action—the expanding roles of ARGONAUTES. *Current Opinion in Plant Biology*, **11**:560–566

Marsolais, F., Hernández-Sebastiá, C., Rousseau, A., and Varin, L. (2004) Molecular and biochemical characterization of BNST4, an ethanol-inducible steroid sulfotransferase from *Brassica napus*, and regulation of BNST genes by chemical stress and during development.

Plant Science **166**:12

Negishi, M., Pedersen, G., Petrotchencko, E., Shevstov, S., Gorokhov, A., Kakuta, Y., and Pedersen C. (2001) Archives of Biochemistry and Biophysics, **309B**: 149-157

Nimmagadda, D., Cherala, G., and Ghatta, S. (2006) Cytosolic sulfotransferases. Indian Journal of Experimental Biology. **44**:171-182

Oñate-Sánchez, L., and Vicente-Carbajosa, J. (2008) DNA-free RNA isolation protocols for *Arabidopsis thaliana*, including seeds and siliques. BMC Research Notes, **1**:93

Piotrowski, M., Schemenewitz, A., Lopukhina, A., Muller, A., Janowitz, T., Weiler, E.W., and Oecking, C. (2004) Desulfoglucosinolate sulfotransferases from *Arabidopsis thaliana* catalyze the final step in the biosynthesis of the glucosinolate core structure. Journal of Biological Chemistry, **279**:50717-50725

Ramachandran, V., and Chen, X. (2008) Small RNA metabolism in Arabidopsis. Trends in Plant Science, **13**:368-374.

Riefler, M., Novak, O., Strnad, M., and Schmulling, T. (2006) *Arabidopsis* cytokinin receptor mutants reveal functions in shoot growth, leaf senescence, seed size, germination, root development, and cytokinin metabolism. Plant Cell **18**: 40-54

Rivoal J, Hanson AD (1994) Choline-O-Sulfate Biosynthesis in Plants (Identification and Partial Characterization of a Salinity-Inducible Choline Sulfotransferase from Species of *Limonium* (Plumbaginaceae). Plant Physiology **106**: 1187-1193

Schwab, R., Ossowski, S., Riestler, M., Warthmann, N., and Weigel, D. (2006) Highly specific gene silencing by artificial microRNAs in *Arabidopsis*. Plant Cell, **18**:1121-33

Sembder, G., Atzom, R., and Schneider, G. (1994) Plant hormone conjugation. Plant Molecular Biology, **26**:1459-1481

Varin, L., Marsolais, F., Richard, M., and Rouleau, M. (1997) Sulfation and

sulfotransferases 6: Biochemistry and molecular biology of plant sulfotransferases. FASEB Journal, **11**: 517-525

Varkonyi-Gasic, E., Wu, R., Wood, M., Alton, E.F., and Hellens, R.P. (2007) Protocol: a highly sensitive RT-PCR method for detection and quantification of microRNAs, Plant Methods, **3**:12

Vaucheret, H. (2006) Post-transcriptional smallRNA pathways in plants: mechanisms and regulations. Genes & Development, **20**:759-771

Wasternack, C. (2007) Jasmonates: An Update on Biosynthesis, Signal Transduction and Action in Plant Stress Response, Growth and Development. Annal Botany, **100**:681-97.

Weinshilboum, R., and Otterness, D. (1994) Sulfotransferase enzymes. Handbook of experimental pharmacology ISSN 0171-2004 112

Xiong, L., Gong, Z., Rock, C.D., Subramanian, S., Guo, Y., Xu, W., Galbraith, D. and Zhu, J.K. (2001) Modulation of abscisic acid signal transduction and biosynthesis by an Sm-like protein in *Arabidopsis*. Developmental Cell, **1**:771–781.

Yang, L., Liu, Z., Lu, F., Dong, A., and Huang, H. (2006) SERRATE is a novel nuclear regulator in primary microRNA processing in *Arabidopsis*. The Plant Journal **47**: 841–850

Yasuda, S., Suik, M., and Liu, M.C. (2005) Oral contraceptives as substrates and inhibitors for human cytosolic SULTs. Journal of Biochemistry, **137**: 401-406

Zimmermann, P., Hirsch-Hoffmann, M., Hennig, L., and Gruissem, W. (2004).

"GENEVESTIGATOR. *Arabidopsis* microarray database and analysis toolbox." Plant Physiology **136**:2621-2632.